

1 **Multi-pollutants emissions from the burning of major**
2 **agricultural residues in China and the related**
3 **health-economic effect assessment**

4 Chunlin Li¹, Yunjie Hu¹, Fei Zhang¹, Jianmin Chen^{1,2}, Zhen Ma¹, Xingnan Ye¹, Xin
5 Yang^{1,2}, Lin Wang^{1,2}, Xingfu Tang¹, Renhe Zhang², Mu Mu², Guihua Wang²,
6 Haidong Kan³, Xinming Wang⁴, Abdelwahid Mellouki⁵

7 ¹Shanghai Key Laboratory of Atmospheric Particle Pollution and Prevention (LAP³), Department
8 of Environmental Science & Engineering, Fudan University, Handan Road 220, Shanghai 200433,
9 China

10 ²Institute of Atmospheric Sciences, Fudan University, Handan Road 220, Shanghai 200433, China

11 ³Public Health School, Fudan University, Dongan Road 120, Shanghai 200032, China

12 ⁴State Key Lab of Organ Geochemistry, Guangzhou Institute of Geochemistry, Chinese Academy
13 of Sciences, Kehuajie Road 511, Guangzhou 510640, China

14 ⁵Institut de Combustion, Aérothermique, Réactivité et Environnement, CNRS, 45071 Orléans
15 cedex 02, France

16 *Correspondence to:* J. M. Chen (jmchen@fudan.edu.cn)

17 **Abstract.** Multi-pollutants in smoke particulate matter (SPM) were identified and
18 quantified for biomass burning of five major agricultural residues such as wheat, rice,
19 corn, cotton, and soybean straws in China by aerosol chamber system combining
20 with various measurement techniques. The primary emission factors (EFs) for PM_{1.0}
21 and PM_{2.5} are 3.04-12.64 and 3.25-15.16 g kg⁻¹. Organic carbon (OC), elemental
22 carbon (EC), water-soluble inorganics (WSI), water-soluble organic acids (WSOA),
23 water-soluble amine salts (WSA), trace mineral elements (THM), polycyclic
24 aromatic hydrocarbons (PAHs), and phenols in smoke PM_{1.0}/PM_{2.5} are
25 1.34-6.04/1.54-7.42, 0.58-2.08/0.61-2.18, 0.51-3.52/0.52-3.81, 0.13-0.64/0.14-0.77,
26 (4.39-85.72/4.51-104.79)×10⁻³, (11.8-51.1/14.0-131.6)×10⁻³, (1.1-4.0/1.8-8.3)×10⁻³,
27 and (7.7-23.5/9.7-41.5)×10⁻³ g kg⁻¹, respectively. BC mainly exist in PM_{1.0}, heavy
28 metal-bearing particles favor to reside in the range of smoke PM_{1.0-2.5}, which are also

29 confirmed by individual particle analysis.

30 With respect to five scenarios of burning activities, the average emissions and
31 overall propagation of uncertainties at 95% confidence interval (CI) of SPM from
32 agricultural open burning in China in 2012 were estimated for PM_{2.5}, PM_{1.0}, OC, EC,
33 WSI, WSOA, WSA, THM, PAHs, and phenols to be 1005.7 (-24.6% , 33.7%), 901.4
34 (-24.4%, 33.5%), 432.4 (-24.2%, 33.5%), 134.2 (-24.8%, 34.0%), 249.8 (-25.4%,
35 34.9%), 25.1 (-33.3%, 41.4%), 5.8 (-30.1%, 38.5%), 8.7 (-26.6%, 35.6%), 0.5
36 (-26.0%, 34.9%), and 2.7 (-26.1%, 35.1%) Gg, respectively. The emissions were
37 further temporal-spatially characterized using geographic information system (GIS)
38 at different regions in summer and autumn post-harvest periods. It was found less
39 than 25% of the total emissions were released during summer harvest that was
40 mainly contributed by the North Plain and the Central of China, especially Henan,
41 Shandong, and Anhui, leading the top three provinces of smoke particle emissions.

42 Flux concentrations of primarily emitted smoke PM_{2.5} that were calculated using
43 box-model method based on five versions of emission inventories all exceed the
44 carcinogenic risk permissible exposure limits (PEL). The health impacts and
45 health-related economic losses from the smoke PM_{2.5} short-term exposure were
46 assessed. The results show that China suffered from 7836 (95% CI: 3232, 12362)
47 premature mortality and 7267237 (95% CI: 2961487, 1130784) chronic bronchitis in
48 2012, which led to 8822.4 (95% CI: 3574.4, 13034.2) million US\$, or 0.1% of the
49 total GDP losses. We suggest that percentage of open burnt crop straws at
50 post-harvest period should be cut down by over 97% to ensure risk aversion from
51 carcinogenicity, especially the North Plain and the Northeast, where the emissions
52 should decrease at least by 94% to meet the PEL. Under such emission control, over
53 92% of the mortality and morbidity attributed to agricultural fire smoke PM_{2.5} can be
54 avoided in China.

55 **Key words:** agricultural straw burning, aerosol chamber, smoke particle, emission
56 factor, emission inventory, health effect, emission control policy

57 **1 Introduction**

58 Biomass burning (BB) is a significant source of particulate- and gaseous- pollutants
59 (Andreae and Merlet, 2001; Clarke et al., 2007; Ram et al., 2011; Saikawa et al.,
60 2009a; Tian et al., 2008). It was estimated that open burning of biomass contributed
61 approximately 40% of the globally averaged annual submicron black carbon (BC)
62 aerosol emissions and 65% of primary OC emissions (Bond et al., 2013). China is
63 the major contributor that bears over 24% of global emissions of carbonaceous
64 aerosols, especially from agricultural field burning, about 0.04~0.5 Tg EC and
65 0.4~2.1 Tg OC are released annually (Bond, 2004; Cao et al., 2006; Qin and Xie,
66 2012; Saikawa et al., 2009), resulting in great radiative forcing, air quality
67 deterioration, visibility reduction, premature mortality, and economic loss regionally
68 and globally (Bølling et al., 2009; Bond et al., 2013; Huang et al., 2014; Janssen et
69 al., 2011; Rosenfeld, 2006; Saikawa et al., 2009; Shindell et al., 2012).

70 BB also represents one of the most uncertainties in the emission, climate effect,
71 and public health assessments, which finally relies on the uncertainties in detailed
72 chemical emissions or related properties and burning activities like strength or
73 percentage of biomass fuel burned (Tian et al., 2008; Andreae and Merlet, 2001;
74 Levin et al., 2010). For example, studies have focused on OC and EC emissions due
75 to their specific optical properties (Bond et al., 2013; Cao et al., 2006; Qin and Xie,
76 2012; Ram et al., 2011). OC like sulfate and nitrate can cool the atmosphere by
77 increasing the Earth's reflectivity, however, smoke OC on the other hand has been
78 treated as brown carbon to exhibit pronounced light absorption character (Chen et al.,
79 2015; Ackerman, 2000; Chakrabarty et al., 2010; Christopher et al., 2000). The
80 coated or internal mixed sulfate or nitrate can act as lens to enhance the light
81 absorption activity of BC (Zhang et al., 2008b), probably also the activity of brown
82 carbon (Chen et al., 2015). However, primary emissions for OC, EC, and alkali
83 components are confused and have a wide range (Sen et al., 2014; Cao et al., 2006;
84 Hayashi et al., 2014), and some study still took OC with negative forcing activity
85 (Saikawa et al., 2009; Shindell et al., 2012). Besides, smoke EC is consisting of soot

86 and char, and soot-EC has a higher light-absorption potential compared to char-EC
87 (Arora and Jain, 2015; Reid et al., 2005a). Division and quantification of char- and
88 soot-EC emissions for biomass burning are understudied (Arora and Jain, 2015; Han
89 et al., 2007, 2009). Moreover, other components like organic acids, amines, phenols,
90 and mineral elements that enable CCN activity or endow health hazard of smoke
91 aerosol are also deficient, variable, or outdated, which may hinder our overall
92 understanding of biomass burning contributions and also atmospheric process of
93 smoke particles (Li et al., 2015; Akagi et al., 2011; Chan et al., 2005; Dhammapala
94 et al., 2007a; Ge et al., 2011; Reid et al., 2005a, b).

95 Studies using carbon mass-balance (CMB) and pollutant concentration-chamber
96 volume quantification are the two common methods to derive the emission factors
97 for biomass burning aerosols (Akagi et al., 2011; Li et al., 2007; Zhang et al., 2008a).
98 Carbonaceous and inorganics components of smoke particles not only vary with
99 biomass issues (fuel types, water content, or burning strength), but also relate to
100 burning condition and environment (flaming or smoldering, field burning or
101 laboratory simulation), extent of aging, sampling methods, and measurement
102 technologies (Grieshop et al., 2009; Hayashi et al., 2014; Reid et al., 2005b).
103 Comparing to field observations that are closer to the actual burning (Li et al., 2007;
104 Akagi et al., 2011; Rose et al., 2011; Saffari et al., 2013), laboratory studies have a
105 definite advantage over field burning research in emission analysis (Jayarathne et al.,
106 2014; Sun et al., 2016; Zhang et al., 2008a). For example, the environment, amount
107 of fuel, and burning conditions can be precisely controlled, the contamination from
108 ambient atmosphere to the emissions can be excluded, and chemical compositions at
109 different aging extent can be quantified using aerosol chamber system (Li et al.,
110 2015, 2016; Aurell et al., 2015; Dhammapala et al., 2007b).

111 The activity rates of biomass burning (burning rate of biomass fuels) are also
112 response to the great uncertainties in the emission estimates (Sun et al., 2016; Zhang
113 et al., 2008a). Seldom study ever focused on the burning rates, and the limited data
114 were treated as simplex constant or dynamic values in many studies of emission
115 estimation in a certain year or for annual variations with a long time scales, thus,

116 significant difference among the results were founded (Qin and Xie, 2011, 2012;
117 Zhang et al., 2011; Zhao et al., 2012). For instance, Cao et al. (2006, 2011) estimated
118 primary smoke carbonaceous materials emissions for 2000 and 2007 in China with
119 same field burning rates, the results were almost the same for the two year with
120 103-104 Gg yr⁻¹ BC and 425.9-433.3 Gg yr⁻¹ OC emitted. He et al. (2011b) found
121 the declining trends in biomass burning emissions in the Pearl River Delta for the
122 period 2003-2007 based on constant activity data of burning rates. Lu et al. (2011)
123 developed primary carbonaceous aerosol emissions in China for 1996-2010 with
124 time-dependent activity rates extrapolated from 2008 to 2010 based on national
125 fast-track statistic, rapid increase of OC and EC emissions were reported, and OC
126 increased from 1.5 to 2.3 Tg yr⁻¹, BC increased from 418 to 619 Gg yr⁻¹. Qin and Xie
127 (2012) estimated BC emission from crop straw open burning for 1980-2009 with
128 variable burning rates based on peasants' income development, the increasing trend
129 in BC emission was also confirmed, and BC emission increased from 4.3 to 116.6
130 Gg yr⁻¹.

131 As most anthropogenic pollutants are concentrated in submicron particulate
132 matters (PM_{1.0}) (Ripoll et al., 2015), more pronounced relationship of ambient PM_{1.0}
133 to haze formation and adverse health effect has been reported (Huang et al., 2003;
134 Roemer et al., 2001; Shi et al., 2014). Nevertheless, associated chemical
135 characterization of PM_{1.0} is still undefined (Li et al., 2015; Safai et al., 2013; Cheng
136 et al., 2006). The study of source-specific PM_{1.0} chemical compositions and
137 emissions are necessary to replenish database for contribution assessment and model
138 application in atmospheric chemistry, climate changes, and public health evaluation.

139 The emission inventories and forecasting in the emissions of atmospheric
140 pollutants have been widely studied, and the incurred mortality, climatic effect, and
141 economic loss have also been estimated (Ostro and Chestnut, 1998; Saikawa et al.,
142 2009; Shindell et al., 2012), based on which the emission control policies were
143 proposed. Shindell et al. (2012) considered ~400 control measures in tropospheric
144 BC and O₃ emissions for the benefit of global or regional human health and food
145 security, and 14 optimal measures targeting CH₄ and BC emissions were identified.

146 Saikawa et al. (2009) compared different scenarios of OC, EC, and sulfate emissions
147 in China in 2030, concluding that maximum feasible reduction may avoid over
148 480000 premature deaths in China and decrease the radiative force from -97 to -15
149 mW m^{-2} globally. Wang et al. (2008a) reported field burning restriction may save
150 about 5 billion dollars losses from biological resource and air pollution. However,
151 the generalized strategies in emission reduction were inadequate and lack actual
152 practicality (Streets, 2007; Lin et al., 2010).

153 In this study, burning experiments with five major agricultural straws were
154 conducted using a combustion stove in combination with an aerosol chamber system.
155 Accurate compositions and emission factors for SPM in $\text{PM}_{1.0}$ and $\text{PM}_{2.5}$ were
156 characterized and established. Afterwards, up-to-date emissions for agricultural open
157 burning aerosol in 2012 were developed, health and health-related economic impacts
158 from smoke $\text{PM}_{2.5}$ exposure were also assessed. Finally, emission reduction strategy
159 that was implemented in field burning rate control for the carcinogenic risk concern
160 was proposed, which should help establish the policy and provide an idea for the
161 emission control.

162 **2 Methodology**

163 An overview of the research procedures including emission factors acquirement and
164 emission inventory calculation is shown in Fig. 1. Tabulation of emission factors is
165 self-established in our laboratory using a combustion stove to simulate open burning
166 and an aerosol chamber to quantify the emissions. Then, we use a bottom-up
167 approach to calculate the emission inventory of agricultural field burning over China
168 mainland based on crop production data in 2012. Emissions for each species are
169 estimated as:

$$170 E_{k,j} = \sum_i A_{k,i} \times EF_{i,j} \quad (1)$$

171 where E_j is emission, $A_{k,i}$ is effective biofuel consumption, and $EF_{i,j}$ is emission
172 factor. k , i , and j indicates region, agricultural residue type, and particulate chemical
173 species.

174 State-of-the art chemical transport and box models were commonly applied to
175 reproduce or simulate the ambient aerosol concentrations (Ram et al., 2011; Reddy
176 and Venkataraman, 2000; Saikawa et al., 2009). In this study, spatio-temporal
177 dynamic box model is used to calculate the emission flux concentration. Regional
178 crop straws are premised to be combusted proportionally only in the fire occurrence
179 days. Dismissing interaction of emitted pollutants in space and time, pollutants will
180 distribute uniformly in a space covering an area of specific region with mixing
181 height of 0.5 km (atmospheric boundary layer). The flux concentration of
182 agricultural burning smoke can be calculated by Eq. (2):

$$183 \quad C_{k,j} = \frac{E_{k,j}}{S_k \times h \times T_k} \quad (2)$$

184 in Eq. (2), $C_{k,j}$ is flux concentration of smoke aerosol, S_k is regional area, h is
185 boundary layer height, T_k is agricultural field fire duration time.

186 **2.1 Aerosol chamber work and emission factors**

187 **2.1.1 Crop straws**

188 Five kinds of representative crop residues were used for the burning experiments, i.e.,
189 wheat, rice, corn, cotton, and soybean straws. The straws were collected based on
190 regional features of agricultural planting, winter wheat straws were collected from
191 Anhui province, late rice straws from Shanghai, corn straws from Henan province,
192 cotton and soybean residues from Xinjiang. All straws were stored under dark, airy,
193 and cooling condition. Prior to the burning experiment, the dirt and weeds were
194 removed, then straws were dehydrated (at 100 °C for 24 h) to minimize effect of the
195 water content on the burning and pollutant emissions, as study found pollutants
196 emissions and combustion efficiencies (CE) are response to water content, increased
197 moisture content enhances the emissions but also alter the chemical compositions of
198 smoke aerosols (Reid et al., 2005b; Aurell et al., 2015; Hayashi et al., 2014).
199 Although straws in the field are not well dried and moisture contents vary with
200 weather, ventilation, and storing times, for the convenience of practical application

201 and comparison of burnings and emissions, water contents of the straws were
202 controlled within 2 wt.%, which has been applied in many studies (Hayashi et al.,
203 2014; Huo et al., 2016; Li et al., 2015; Oanh et al., 2011; Zhang et al., 2008a, 2011).
204 The dry straws were then cut to a length of approximately 10 cm and weighted 10.0
205 g per serving.

206 **2.1.2 Burning experiments**

207 The experiments were conducted using an aerosol chamber system (Fig. S1 in
208 supplement information, SI), which was loaded in a temperature-controlled room
209 (18-22 °C, 40%-60% RH). A stainless combustion stove was self-designed to simulate
210 typical field burning of crop straws by automatic ignition with LPG (Liquid
211 petroleum gas) in particular, albeit on a small scale (ignition time less than 0.1 s).
212 10.0 g conditioned residues were sealed in the 0.227 m³ combustion stove in
213 advance, once ignited, the force-ventilation and HEPA filtrated particle-free air were
214 supplied (300 L min⁻¹). The emissions were immediately injected into a clean,
215 evacuated aerosol chamber. The burning last about 1 min and over 1 m³ particle-free
216 air flushed the stove to ensure all the emissions were transferred into the chamber.

217 The chamber was custom-built to quantify the emissions and characterize the
218 physiochemical properties of smoke aerosols, detailed description of the chamber
219 can be found elsewhere (Zhang et al., 2008a, 2011; Li et al., 2015, 2016). Briefly, the
220 chamber has a volume of 4.5 m³ with 0.3 mm Teflon coating on the inner side, a
221 magnetic fan fixed on the bottom to stir the aerosol uniformly, and a hygroclip
222 monitor (Rotronic, Model IM-4) equipped inside the chamber to measure the
223 temperature and relative humidity of the aerosol. Before experiment, the chamber
224 was flushed with particle-free air for 6 h, oxidized by high concentration ozone (~3
225 ppm) for 12 h, then flushed and vacuumized, filled with pure dry air to 80 KPa for
226 use. The emissions from straw burning were aspirated into the chamber till room
227 pressure, afterwards, size measurement and sampling of smoke aerosols were
228 conducted from the chamber. For each type of straw, four burning experiments were

229 conducted. The unburned residues were weighted and deducted from 10.0 g after
230 each test.

231 Modified combustion efficiency (MCE) for each burning was monitored with CO
232 and CO₂ measuring to determine the burning phase and to ensure the repeatability.
233 MCE is defined as $\Delta\text{CO}_2/(\Delta\text{CO}_2+\Delta\text{CO})$, where ΔCO_2 and ΔCO are the excess molar
234 mixing ratios of CO₂ and CO (Reid et al., 2005b). A gas-chromatograph (GC, model
235 930, Shanghai, Hai Xin Gas Chromatograph Co., LTD) equipped with a flame
236 ionization detector, an Ni-H convertor, and a stainless steel column (2 m long)
237 packed with 15% DNP was used to measure CO and CO₂ concentrations in the
238 chamber. And MCE were 0.89-0.96 for all the experiments (see in SI, Table S1),
239 indicating flaming combustion dominated, which were comparable to that in the
240 field burning (Li et al., 2003; Li et al., 2007).

241 **2.1.3 Size and morphology of smoke aerosol**

242 Size distribution (10 nm-10 μm) of smoke particles was measured using a
243 Wide-range Particle Spectrometer (WPS, Model 1000XP, TSI, USA), which has
244 been described by Li et al (2015). Briefly, WPS integrates the function of scan
245 mobility particle sizer (SMPS) and laser particle sizer (LPS), 0.3 L min⁻¹ flow is
246 introduced to SMPS part to classify mobility size from 10 nm to 500 nm in 48 bins,
247 and 0.7 L min⁻¹ flow is introduced to LPS part to measure aerodynamic diameter
248 from 350 nm to 10 μm in 18 bins. Particle density, refractive index, and scanning
249 time were set as 1.0 g cm⁻³, 1.45, and 3 min loop⁻¹, respectively, and charge
250 correction mode was on for the measurement. A diffusion dryer tube (45 cm in
251 length) filled with descant-silica gel was set prior to the inlet of WPS. Before
252 experiment, WPS was calibrated with certified polystyrene latex spheres (PSL, 40,
253 80, and 220 nm, Duke Scientific).

254 SPM from the 5 types crop straws burning were sampled onto copper grids coated
255 with carbon film (carbon type-B, 300-mesh copper, Tianld Co., China) using a
256 single-stage cascade impactor with a 0.5 mm diameter jet nozzle at a flow rate of 1.0

257 L min⁻¹. The sampler has a collection efficiency of 100% at 0.5 μm aerodynamic
258 diameter. More information about the cascade impactor can be found elsewhere (Fu
259 et al., 2012; Hu et al., 2015). Then, a JEOL-2010F field emission high-resolution
260 transmission electron microscope (FE-HRTEM) coupled with an oxford
261 energy-dispersive X-ray spectrum (EDX) was applied to investigate the morphology,
262 composition, and mixing state of individual particles.

263 **2.1.4 Chemical sampling and analysis**

264 PM_{1.0} and PM_{2.5} samples for each burning were collected onto pretreated quartz filter
265 of 90 mm in diameter (Tissuquartz, Pall Corp., USA) from the chamber using a
266 high-volume Particle Sampler (HY-100, Qingdao Hengyuan S.T. Development Co.,
267 Ltd) operating at 100 L min⁻¹. Each filter sampling duration time is 5 min, and total
268 44 samples (including 4 blank samples) were gathered. The quartz microfiber filters
269 were prebaked for 8 h at 450 °C to eliminate contamination. Before and after the
270 sampling, the filters were weighted using a balance (Sartorius BP211D) with an
271 accuracy of 10 μg, and the filters were balanced in an electronic desiccator (40 %
272 RH, 22 °C) for 24 h before usage. After weighting, the loaded filters were stored at
273 -20 °C in a refrigerator for further analysis.

274 Water soluble species including general inorganic ions (ions: F⁻, Cl⁻, NO₂⁻, NO₃⁻,
275 SO₄²⁻, Na⁺, NH₄⁺, K⁺, Ca²⁺, Mg²⁺), organic acids (CH₃COOH, HCOOH, C₂H₂O₄,
276 CH₃SO₃H), and seven protonated amines (MeOH⁺, TeOH⁺, MMAH⁺, DMAH⁺,
277 TMAH⁺, MEAH⁺, and DEAH⁺ for short, corresponding to monoethanolaminium,
278 triethanolaminium, monomethylaminium, dimethylaminium, triethylaminium,
279 monoethylaminium, and diethylaminium) were measured from 1/4 of each filter
280 with ion chromatography (IC, Model 850 Professional IC, Metrohm, USA) consists
281 of a separation column (Metrosep A Supp 7 250/4.0 for anion and organic acids,
282 Metrosep C-4 150/4.0 for cation, and Metrosep C4-250/4.0 for water soluble
283 aminiums). Sampled filters were ultrasonically extracted with 15.0 mL deionized
284 water (Mili-Q water, 18.2 MΩ cm), extracted solutions were filtrated using 0.2 μm

285 filters before injected into IC for measurement. Detection limits (DLs) for the ions
286 and aminiums were within 0.5~3.5 ng mL⁻¹, the correlation coefficients for all
287 calibration curves were better than 0.99, and recovery rates for aminiums were in the
288 range of 93%~106% (see in SI, Table S2). Details for the aminium measurements
289 can be found in the work of Tao et al. (2016).

290 1/4 of each filter was acid dissolved to measure the selected elements (As, Pb, Cr,
291 Cd, Ni, V, Zn, Al), of which As, Zn, Pb, Cr, Cd, and Ni are USEPA priority
292 controlled pollutants (Wu et al., 2011). The smashed filters were digested at 170 °C
293 for 4 h in high-pressure Teflon digestion vessel with 3.0 mL concentrated HNO₃, 1.0
294 mL concentrated HClO₄, and 1.0 mL concentrated HF. Afterwards, the almost dry
295 solution was diluted and characterized using Inductively Coupled Plasma Optical
296 Emission Spectrometer (ICP-OES, Atom Scan 2000, JarroU-Ash, USA). The
297 following wavelength lines of the ICP-OES analysis were used: As 189.042, Pb
298 220.353, Cd 228.802, Cr 205552, Ni 231.604, V 311.071, Zn 206.191, and Al
299 394.401. All reagents used were of highest grades, and recovery tests were
300 conducted with standard additions, recoveries of each element were in the range of
301 93%~102% (see in SI, Table S2).

302 Another 1/4 of each filter was ultrasonically double extracted with 15.0 mL
303 HPLC-grade CH₂Cl₂. The extracts were then condensed with rotary evaporator and
304 quantified to 1.0 mL. 16 targeted PAHs (2-ring, naphthalene (Nap); 3-ring,
305 acenaphthylene (Ac), acenaphthene (Ace), fluorene (Fl), phenanthrene (Phe),
306 anthracene (Ant); 4-ring, fluoranthene (Flu), pyrene (Pyr), benzo[a]anthracene (BaA),
307 chrysene (Chr); 5-ring, benzo[b]fluoranthene (BbF), benzo[k]fluoranthene (BkF),
308 benzo[a]pyrene (BaP), dibenzo[a,h]anthracene (DBA); and 6-ring: indeno[1,2,3-cd]
309 pyrene (IP), benzo[ghi]perylene (BghiP)) and 5 selected phenols (phenol,
310 2-methoxyphenol, 4-ethylphenol, 4-ethyl-2-methoxyphenol, 2,6-dimethoxyphenol)
311 were measured from the concentrated extracts using an Agilent 6890 Series gas
312 chromatography system coupled with a HP 5973 Mass Selective Detector (GC-MS,
313 Agilent Technologies, Wilmington DE) . A DB-5ms (30 m × 0.32 mm × 0.25 mm,
314 Agilent 123-5532) column was installed. The temperature programs were presented

315 as follows: initially at 40 °C, hold for 4 min, to 150 °C at 20 °C min⁻¹, then to 280 °C
316 at 5 °C min⁻¹, hold for 10 min. The interface temperature was kept at 280 °C, the MS
317 was operated in electron impact mode with an ion source temperature of 230 °C, and
318 the high-purity helium (99.999%) carrier gas was maintained at a constant pressure
319 of 16.2 psi with a flow of 2.0 mL min⁻¹. The calibration curves were optimized to be
320 better than 99.9%. Prior to the measurements, PAHs and Phenols recovery studies
321 were undertaken, and recoveries were acceptable with rates of 82%~99% (see in SI,
322 Table S2). In addition, Phenanthrene-d10 (Phe-d10) as internal standard surrogate
323 was added into the PAHs mixture, recovery rate of which was 94%.

324 Organic carbon (OC) and elemental carbon (EC) were measured with the rest
325 quartz filters using a carbon analyzer (Sunset laboratory Inc., Forest Grove, OR)
326 based on the thermal-optical transmittance (TOT) method with a modified
327 NIOSH-5040 (National Institute of Occupational Safety and Health) protocol. Four
328 organic fractions (OC1, OC2, OC3, and OC4 at 150, 250, 450, and 550 °C,
329 respectively), PC fraction (a pyrolyzed carbonaceous component determined when
330 transmitted laser returned to its original intensity after the sample was exposed to
331 oxygen), and three EC fractions (EC1, EC2, and EC3 at 550, 700, and 800 °C,
332 respectively) are produced. And OC is technically defined as OC1 + OC2 + OC3 +
333 OC4 + PC, while EC is defined as EC1 + EC2 + EC3 - PC (Seinfeld et al., 2012).
334 The instrument detection limits for total OC and EC that deposit on the filter are 0.25
335 and 0.12 µg C cm⁻². The quality of the data above was guaranteed by standard
336 materials calibration, recovery rate, and operational blank correction. And blank
337 levels were less than 5% of the measured values for all the species.

338 **2.1.5 Calculation of emission factors**

339 The emission quantities derived from the experiment were converted into quantities
340 per unit weight of initial residues as emission factor (EF, unit: g kg⁻¹), which can be
341 calculated from the direct method with effective filter sampling weight, chamber
342 volume, and effective amount of crop straw consumed (Dhammapala et al., 2006,

343 2007a, b; Zhang et al., 2008a), or alternatively from the carbon mass balance method
344 (CMB) via conservation of Carbon in biomass, disregarding the weight of biomass
345 that burnt (Dhammapala et al., 2006; Li et al., 2007). EFs determined from these two
346 methods were found to be in good agreement (Dhammapala et al., 2006),
347 nevertheless, CMB method needs more auxiliary information (e.g., concentrations of
348 CO, CO₂, CH₄, non-methane hydrocarbons, and also particulate carbons), which
349 may result in data redundancy and uncertainty propagation, hence we applied the
350 direct method to calculate EFs in this work. To be more accurate, influence of wall
351 loss and makeup air dilution on smoke particles sampling from the chamber were
352 considered and corrected, details see in SI.

353 In this study, duration for each test (burning, chamber condition, size
354 measurement, and filter sampling) was controlled within 20 min, therefore, the
355 physicochemical processes of pollutants in the chamber can be negligible, and
356 smoke aerosols we measured were primary emissions.

357 **2.2 Emission inventory calculation**

358 **2.2.1 Agricultural field fire survey**

359 Fire sites over China from 2011 to 2013 were statistically analyzed, and the data of
360 mainland agricultural fire sites was derived from the daily report of the Ministry of
361 Environmental Protection of China (MEPC) (website: <http://hj.mep.gov.cn/jgjs/>).
362 Agricultural fire sites were screened out from MODIS (Moderate Resolution
363 Imaging Spectroradiometer) daily fire products (1 km × 1 km resolution level 3
364 hotspot) using a high resolution real time land use based on geography information
365 system (GIS). Spatial and temporal distributions of fire sites were displayed in Fig.
366 S2 (SI), over 5000 fire sites were allocated into two prominent burning periods
367 corresponding to summer (May to July) and autumn (September to November)
368 harvests, and filed burning last 54 days and 60 days on statistical average during the
369 two harvests. In the North of China, open burning occurred primarily in autumn,
370 while temporal-character of field fires was not obvious in the North Plain and the

371 Center of China, where field fires can be observed frequently during the whole
372 investigation time.

373 **2.2.2 Crop straw production**

374 Crop straw production was generally derived from annual or monthly crop production
375 by multiplying crop-specific ratios of residue-to-production (He et al., 2011b; Cao et
376 al., 2011; Zhao et al., 2012). In this study, crop productions were furtherly classified
377 into summer harvest and autumn harvest productions according to field fire sites
378 analysis and traditional seasonal planting and harvesting. The amount of straw
379 produced was calculated by Eq. (3):

$$380 \quad M_{t,k,i} = P_{t,k,i} \times r_i \times H_{t,k,i} \times D_i \quad (3)$$

381 in which M is mass of crop straws produced; P is annual crop-specific amount of
382 crop production; r is the residue-to-production ratio; D is the dry matter
383 content; $H_{t,k,i}$ is production ratio of crop i at region k during summer or autumn
384 harvest period t .

385 Province-level crop production data of wheat, rice, corn, cotton, and soybean were
386 taken directly from the China Yearbook 2013 (National Bureau of Statistics of China,
387 NBSC, 2013). Crop-specific residue-to-production ratios were cited from Chinese
388 Association of Rural Energy Industry (Wang and Zhang, 2008; data available at
389 <http://www.carei.org.cn/index.php>, in Chinese). Dry matter contents of crop straws
390 were referred to He et al. (2011b) and Greenhouse Gas Inventory Reference Manual
391 (IPCC, 2007). The parameters of residue-to-production ratios and dry matter
392 contents were summarized in Table S3 (SI). The regional crop production ratios in
393 summer and autumn harvests were listed in Table S4 (SI).

394 **2.2.3 Field burning rate**

395 Uncertainty of emission estimations mostly relies on intangibility of straw open
396 burning rate (Zhao et al., 2012; He et al., 2011b). However, regional or national
397 percentage of straw open burned was seldom studied, and the limited data were

398 outdated and variable. The available studies indicate national field burning rate of
399 crop straws range from 15.2% to 27.2% in China (Daize, 2000; Wei et al., 2004;
400 Zhang et al., 2008a), and more detailed studies indicate about 31.9% of the crop
401 straw burned in the Pearl River Delta from 2003 to 2007 (He et al., 2011b), while the
402 corresponding figures were almost 100% for the Huabei region in 2003 (Zhao et al.,
403 2012). Two versions of province-level field burning rates were commonly used, one
404 was from Cao et al. (2005; 2006; 2011) who deduced the rates based on regional
405 economic level, and the proposal of the rates to be proportional to peasants' income
406 was confirmed later, the rates were first used to calculate open burning emission in
407 2000. The other version was reported by Wang and Zhang (2008), they obtained
408 provincial percentage of residue open burnt via filed survey in 2006. Herein, the two
409 versions were both applied directly into the emission estimation of 2012 in this work
410 and named as business-as-usual scenarios (BAU, BAU-I from Cao et al. and BAU-II
411 from Wang and Zhang in specific).

412 In fact, the burning rates should be dynamic parameters that been influenced by
413 industrial structure, government policy orientation, or public awareness. With crop
414 yields increase and energy consumption structure changes in rural areas, more straws
415 will be discarded and burnt in the field. Nonetheless, rigorous agricultural fire policy
416 may still suppress the condition worsen as it worked during 2008 for Beijing
417 Olympics and 2010 for Shanghai Expo (Huang et al., 2013; Cermak and Knutti,
418 2009; Wang et al., 2010). Qin and Xie (2011; 2012) ever deduced year specific open
419 burning rates in different zone for the period of 1980-2009 according to their
420 respective peasant income changes in a certain year on the basis of peasant income
421 and burning rates in 2006. However, the simple linear relationship should be doubted,
422 as great increase in per capita income after 2006 will surely overestimate the burning
423 rates. We supposed that the burning rates were inverse proportional to peasants'
424 agricultural income proportion (AIP), without considering the policy or potential
425 gain or loss related to agricultural residue treatment. Thus the burning rates
426 established in 2000 and 2006 from Cao et al. (2005) and Wang and Zhang (2008) can
427 be converted into that of 2012 based on economic data from equation below:

$$R_{k,2012} = \frac{I_{k,2012}}{AI_{k,2012}} \times \frac{AI_{k,y}}{I_{k,y}} \times R_{k,y} \quad (4)$$

where R is agricultural straw filed burnt rate, $I_{k,y}$ is peasants' annual income, $AI_{k,y}$ is peasants' annual agricultural income. y indicates reference year (2000 for BAU-I, and 2006 for BAU-II). $I_{k,y}$ and $AI_{k,y}$ can be found or calculated from China Yearbook and China Rural Statistic Yearbook (NBSC, 2004-2013).

The versions of converted rates based on primary industry level were called Economic Models I and II (EM -I and EM-II in short) corresponding to BAU-I and BAU-II. Besides, in 2013, the National Development and Reform Commission of China published the Chinese agricultural straw treatment report of 2012 (NDRC, [2014] No.516, data available at <http://www.sdpc.gov.cn/>, in Chinese) for the first time. The percentages of crop residues discarded in the report were applied in our estimation, which was called NDRC version.

2.2.4 Emission and flux concentration

From above study, emission of SPM pollutants can be calculated by recount of Eq. (1) to get Eq. (5) as it was showed below:

$$E_{t,k,j} = \sum_i M_{t,k,i} \times R_k \times f_i \times EF_{i,j} \quad (5)$$

where $E_{t,k,j}$ is emission amount of chemical species j at region k during harvest period t ; f_i is burning efficiency, the crop specific values were cited as 0.68 for soybean residue and 0.93 for the rest four straws (Zhang et al., 2011; Wang and Zhang, 2008; Zhang et al., 2008a; Koopmans et al., 1997). Thus, flux concentration of corresponded pollutants can be also assessed from box model as mentioned in front.

2.3 Estimate health impacts and health-related economic losses

2.3.1 Carcinogenic risk of Smoke Particulate Matter (CR_{SPM})

Apart from the enormous climatic effects of smoke particle emissions, new

453 epidemiological and toxicological evidence have also linked carbonaceous aerosol to
454 cardiovascular and respiratory health effects according to the World Health
455 Organization (Bruce et al., 1987; IPCC, 2007). Here, we present the fuel-specific
456 carcinogenic risk of SPM (CRSPM, unit: per $\mu\text{g m}^{-3}$) to assess health hazard from
457 agricultural straw burning particles and help source-specific air quality control. The
458 cancer risk attributed to inhalation exposures of smoke $\text{PM}_{2.5}$ from crop straw i
459 burning was calculated as:

$$460 \quad \text{CR}_i = \sum_j f_j \times \text{UnitRisk}_j \quad (6)$$

461 where f_j is mass fraction of individual species j in smoke $\text{PM}_{2.5}$, UnitRisk_j is
462 corresponded unit carcinogenic risk value of species j extracted from database
463 provided by the Integrated Risk Information System (IRIS), California
464 Environmental Protection Agency (CEPA), and related documents (Bruce et al.,
465 1987; Burkart et al., 2013; Tsai et al., 2001; Wu et al., 2009, 2011).

466 CR_i is estimated based on dose addition model of selected hazardous air
467 pollutants (HAPs) including USEPA priority pollutants of PAHs and heavy metals.
468 And UnitRisk values of the selected HAPs presented in Table S5 (SI). Synergistic
469 interactions among pollutants are dismissed, albeit possible. The cancer risk of
470 chromium is adjusted by multiplying a factor of 0.2, assuming that only 20% Cr
471 measured is in the toxic hexavalent form (Bell and Hipfner, 1997). Benzo[a]pyrene
472 (BaP) is used as an indicator compound of carcinogenicity, legally binding threshold
473 of BaP in most countries ranges from 0.7 to 1.3 ng m^{-3} , corresponded carcinogenic
474 risk of BaP is about 1.1×10^{-6} per ng m^{-3} (Bruce et al., 1987; Burkart et al., 2013).
475 Thus, one in million level of carcinogenic potential is frequently used to identify
476 risks of concern in public health and environmental decision making, and
477 permissible exposure limits (PEL, unit: $\mu\text{g m}^{-3}$) of crop straw burning particles can
478 be estimated as:

$$479 \quad \text{PEL}_i = \frac{10^{-6}}{\text{CR}_i} \quad (7)$$

480 2.3.2 Human exposure and health impacts

481 Robust relationship between surface PM_{2.5} and health effects has been revealed and
482 confirmed by many studies (Pope et al., 2004; Wong et al., 2008). PM_{2.5}-related
483 health endpoints are composed of a range of elements from sub-clinical effects to the
484 onset of diseases and the final death (Davidson et al., 2005). In this study, incidence
485 of commonly studied endpoints like premature mortality, respiratory and
486 cardiovascular hospital admissions, and chronic bronchitis from primary emitted
487 smoke PM_{2.5} short-term exposure were assessed using the Poisson regression model,
488 shown as below (Guttikunda and Kopakka, 2014):

$$489 \Delta E = \Delta \text{Pop} \times \text{IR} \times \left(1 - \frac{1}{e^{\beta \times \Delta C}}\right) \quad (8)$$

490 where ΔE represents the number of estimated cases of mortality and morbidity, ΔC
491 is the incremental concentration of particulate matter (PM) or flux concentration;
492 ΔPop is the population exposed to the incremental particulate concentration of ΔC ;
493 IR is short for incidence rate of the mortality and morbidity endpoints, and β is the
494 coefficient of exposure-response function, defined as the change in number case per
495 unit change in concentration per capita.

496 Concentration-response function and incidence rate of each health endpoint are
497 important in health impacts evaluation and they have variation for different
498 population and regions (Yang et al., 2012; Wong et al., 2008). Here, the variance for
499 sex and ages were neglected. Region-specific exposure-response coefficients for
500 individual mortality were summarized from previous studies, as presented in Table
501 S6 (SI). The coefficients for individual respiratory and cardiovascular hospital
502 admission, and chronic bronchitis were cited as 1.2%, 0.7%, and 4.4% (per 10 μg
503 m^{-3} , 95% CI) from Aunan and Pan's work (Aunan and Pan, 2004). This is the case
504 because seldom studies ever confirmed these topics in China. Region-specific
505 mortality and hospitalization IRs were taken from statistical reports authorized by
506 National Health and Family Planning Commission of the People's Republic of China
507 (NHFPC, 2013), and morbidity of chronic bronchitis were defined as 13.8 % based

508 on the forth national health survey, which was released by the Chinese Ministry of
509 Health in 2008 (CMH, 2009).

510 **2.3.3 Economic valuation of the health impacts**

511 The economic losses of the health impacts associated with smoke PM_{2.5} exposure in
512 2012 were further evaluated. The amended human capital (AHC) approach was
513 employed to calculate the unit economic cost of premature mortality. The commonly
514 applied AHC method uses per capita GDP to measure the value of a statistical year
515 of life (IBRD and SEPA, 2007) based on Eq. (9). It can be used as a social statement
516 of the value of avoiding premature mortality and estimates human capital (HC) from
517 the perspective of entire society, neglecting individual differences (Hou et al., 2012).

$$518 \quad HC_k = \frac{GDP_k}{POP_k} \times \sum_{i=1}^{\tau} \frac{(1+\alpha)^i}{(1+\gamma)^i} \quad (9)$$

519 GDP_k and POP_k are gross domestic production and population of target region k
520 that were reported in the statistical yearbook in 2012; α and γ are economic
521 parameters referring to national GDP growth rate and social discount rate, which
522 were 7.7% and 8.0% in 2012 from National Bureau of Statistics of China (NBSC,
523 2013, data available at <http://www.stats.gov.cn/tjsj/ndsj/>, in Chinese). τ is the
524 life-expectancy lost due to aerosol pollution, and 18 years of life was widely applied
525 (Hou et al., 2012). The annual exchange rate of US dollar to RMB was 6.31 in 2012.
526 One can deduce the HC values of the provinces, municipalities, and autonomous
527 regions in the country, and the calculated regional HC values were listed in Table S7
528 (SI). In this paper, the cost of respiratory, cardiovascular hospital admissions, and
529 chronic bronchitis were 632.2, 1223.4, and 948.6 US\$ per case in 2012, which were
530 derived from the national health statistical reports (NHFPC, 2013).

531 The regional and national health-related economic loss from smoke PM_{2.5}
532 exposure can be calculated based on the excess mortality and morbidity multiplied
533 by the corresponding unit economic values.

534 **3 Result**

535 **3.1 Particulate chemical compositions and emission factors**

536 **3.1.1 Organic carbon and elemental carbon**

537 An overview of particulate chemical compositions for smoke $PM_{2.5}$ and $PM_{1.0}$ is
538 pie-graphically profiled in Fig. 2, and the corresponded emission factors are given in
539 Table 1-2 (detailed EFs for elements, PAHs, and Phenols in Table S8 and S9, SI).
540 From multivariate statistical analysis ($P < 0.05$ at 95% CI), significant differences of
541 chemical compositions and emissions in size range and fuel types can be observed,
542 implying the nonuniform mixing and distribution of particulate pollutants from
543 biomass burning, which is consistent with the conclusion from Lee et al. (2015) and
544 Giordano et al. (2015). EFs of particulate species from this study were compared
545 with that from literature as summarized in Table 3, since EFs in smoke $PM_{1.0}$ were
546 seldom reported, only smoke $PM_{2.5}$ or total particulate matter emissions were
547 collected, which were comparable with the results in this work. EFs of smoke $PM_{2.5}$
548 and $PM_{1.0}$ were in range of 3.25~15.16 and 3.04~13.20 $g\ kg^{-1}$ for the five kinds of
549 crop straws, a high ratio of $PM_{1.0}/PM_{2.5}$ was observed to be over 90 wt.%, which was
550 in line with size distribution analysis of smoke particles given in Fig. S3 (SI). Li et al.
551 (2007) measured the emissions from field burning of crop straws via CMB method,
552 $PM_{2.5}$ EFs for wheat and corn straw were estimated to be 7.6 ± 4.1 and $11.7 \pm 1.0\ g\ kg^{-1}$
553 kg^{-1} (dry basis, MCE > 0.9), which were higher and presented more uncertainties
554 than our result. As study ever found a positive relationship between particulate EFs
555 and moisture content of agricultural residue (Hayashi et al., 2014), it was reasonable
556 that combustion of the dehydrated crop straw produced less smoke aerosol in this
557 work. Hayashi et al. (2014) measured particulate EFs to be 2.2 and 15.0 $g\ kg^{-1}$ for
558 rice and wheat straw of ~10 wt.% moisture content, while corresponded EFs
559 increased to 9.1 and 19.5 $g\ kg^{-1}$ when water content of straw was ~20 wt.%, and the
560 linear equations between smoke EFs and straw moisture content were furtherly
561 proposed. However, the simple linearity and its application scope should be doubted,

562 as Hayashi et al. only considered two water content levels (10 wt.% vs 20 wt.%) and
563 disregarded influence of combustion efficiency for the fires. PM_{2.5} EFs given by
564 Dhammapala et al (2006, 2007a, b) were $4.7 \pm 0.4 \text{ g kg}^{-1}$ for wheat straw and $12.1 \pm$
565 1.4 g kg^{-1} for herbaceous fuel that were burnt using a chamber under flaming phase,
566 and negative response for particulate EFs to combustion efficiency was observed.
567 After all, smoke EFs vary with fires depend on fuel type and moisture, combustion
568 phase, environmental conditions, and some other variables (Reid et al., 2005b).

569 The carbonaceous materials (Organic matter and EC) are dominated in SPM,
570 accounting for about 73.4 wt.% for PM_{2.5} and 71.3 wt.% for PM_{1.0} on average.
571 Organic matter (OM) was converted from OC by multiplying a factor of 1.3 to
572 account for noncarbon materials like oxygen, hydrogen, and other minor species (Li
573 et al., 2007; Li et al., 2015), and Li et al. (2016) ever measured OM/OC ratio as ~1.3
574 for fresh smoke particles via volatility analysis. EFs of EC and OC from this work
575 were consistent with most studies, average OC EFs were 4.21 and 3.58 g kg^{-1} in
576 smoke PM_{2.5} and PM_{1.0}, and the corresponded EC EFs were 1.09 and 1.01 g kg^{-1} ,
577 respectively. These values fell within the ranges (0.9~9.3 g kg^{-1} for OC and 0.2~1.7
578 g kg^{-1} for EC) found in other similar sources (Dhammapala et al., 2007; Hayashi et
579 al., 2014; Li et al., 2007; May et al., 2014). Due to the technical limitation and
580 ambiguous artificial boundary, carbon contents of biomass burning particles have
581 vast variability and uncertainty (Lavanchy et al., 1999; Levin et al., 2010). It was
582 ever reported chamber burn study may overestimate EC EFs due to a misassigned
583 OC-EC split for the heavily mass loaded filter samples (Dhammapala et al., 2007b).
584 Moreover, carbon measurement based on TOT method with NIOSH protocol may
585 overestimate OC fraction by sacrificing EC part compared with that of TOR
586 (Thermal-Optical Reflectance) method with IMPROVE program (Han et al., 2016).
587 Mass ratio of OC/EC is a practical parameter to indicate the primary organic aerosol
588 (OA) emission and secondary organic aerosol (SOA) production. The ratio is
589 influenced by burning conditions, source, aging extent, and particle size (Engelhart
590 et al., 2012; Grieshop et al., 2009). Smoke emitted from smoldering fires is
591 OC-dominated while flaming combustion produces more EC, and the discrepancy of

592 OC/EC ratio can be an order of magnitude regarding to different combustion phase
593 (Grieshop et al., 2009). SOA production upon photo-oxidation will enlarge OC/EC
594 ratio, and positive relation between oxidation level of OA loading and OC/EC ratio
595 was reported (Grieshop et al., 2009). Here, OC/EC ratio in primary emissions varied
596 from 2.4 to 6.2 under flaming phase, similar to previous studies (Arora and Jain,
597 2015; Dhammapala et al., 2007a, b; Hayashi et al., 2014; Lewis et al., 2009). The
598 OC/EC ratios were larger in PM_{2.5} with average value of 3.8, while it was 3.6 in
599 PM_{1.0}, indicating more EC resides in PM_{1.0}.

600 **3.1.2 Water soluble organic acids**

601 Smoke particles comprise a considerable amount of water soluble organic acids
602 (WSOA), it was 3.35 wt.% in PM_{2.5} and 3.17 wt.% in PM_{1.0} on average, which was
603 in line with previous work that organic acids measured represent less than 5 wt.% of
604 the total smoke aerosol mass load and favor to partition in larger size (Falkovich et
605 al., 2005; Gao et al., 2003). Acetic acid followed by methysulfonic acid contributed
606 the most of the measured low molecule weight acids. Oxalic acid is the dominated
607 dicarboxylic acids measured in the ambient environment and biomass burning
608 aerosol (Falkovich et al., 2005; Kundu et al., 2010), and oxalic acid EF was
609 measured to be 2.2 ~ 4.8 and 1.6 ~ 3.6 mg kg⁻¹ for smoke PM_{2.5} and PM_{1.0} in present
610 work. The sums of WSOA EFs ranged from 46.7 to 770.0 mg kg⁻¹. Correlation
611 among the multi-pollutants was analyzed by relevance matrix as shown in Table S10
612 (SI), the strong positive linear relationship ($R^2 > 0.99$, $p < 0.05$ at 95% CI) between
613 WSOA and emissions of OC and PM was observed. Study has confirmed organic
614 acids contribute a significant fraction of both oxygenated volatile organic
615 compounds (OVOCs) in gaseous phase and SOA in particulate phase, the direct
616 emission of particulate organic acids from biomass burning also represents a
617 significant source of precursors for SOA formation, as the low molecular organic
618 acids will evaporate into gas phase or involve in the heterogeneous reaction directly
619 (Takegawa et al., 2007; Veres et al., 2010; Yokelson et al., 2007; Carlton et al., 2006).

620 Moreover, as the significant fraction of water soluble organic carbon, organic acids
621 play major response to CCN activity of smoke particles, and organic acids coating or
622 mixing can amplify hygroscopic growth of inorganic salts by decreasing the
623 deliquescence RH, enable the particle to be CCN at relative low degree of
624 supersaturation (Falkovich et al., 2005; Ghorai et al., 2014). In the ambient
625 environment, organic acids can enhance atmospheric new particle formation by
626 impairing nucleation barrier (Zhang et al., 2004), besides, particulate organic acids
627 can also mobilize the solubility of mineral species, like iron, altering the chemical
628 process of particles (Cwiertny et al., 2008). And prominent optical properties of
629 organic acids like humic/fulvic substance make them as potential contributors to the
630 global warming (Yang et al., 2009; Andreae and Gelencsér, 2006).

631 **3.1.3 Water soluble aminiums**

632 Interest has been focused on the vital role of amines in particle nucleation-growth
633 process and acidity regulating due to their strong base (Tao et al., 2016; Bzdek et al.,
634 2010, 2011). Though ultratrace gaseous amines and particulate aminiums were on
635 the order of pptv or ng m^{-3} , aminium salts exhibit potential climatic and health effect
636 due to their significant different properties in hygroscopicity, optics, and also
637 toxicology (Qiu and Zhang, 2012; Qiu et al., 2011; Samy and Hays, 2013; Zheng et
638 al., 2015; Ho et al., 2015; Tao et al., 2016). It ever proposed that biomass burning is
639 an important source for gaseous amines, especially from smoldering burning, and
640 alkyl amides can be served as biomarkers in particular (Ge et al., 2011; Ho et al.,
641 2015; Lee and Wexler, 2013; Lobert et al., 1990; Simoneit et al., 2003). However,
642 seldom study ever quantitatively explored the particulate water soluble amine salts
643 (WSA) in primary smoke emissions (Schade and Crutzen, 1995; Ge et al., 2011).
644 From this study, WSA contributed about 4.81 wt.% of smoke $\text{PM}_{2.5}$ and 4.69 wt.%
645 of $\text{PM}_{1.0}$, implicating aminium favored to be abundant in fine-mode of smoke
646 particles, especially in $\text{PM}_{2.5-1.0}$. DEAH^+ , TMAH^+ , TEOH^+ and DMAH^+ made up
647 over 80 wt. % of the measured WSA. Fuel-dependence of WSA distribution and

648 emissions were evident. EFs of WSA ranged from 4.5 to 104.8 mg kg⁻¹ in smoke
649 PM_{2.5}, the least was from burning of soybean straw and the largest from cotton and
650 rice straws. We used mass ratio of WSA to NH₄⁺ to denote the enrichment of
651 aminium in particulate phase. Statistical analysis showed WSA/NH₄⁺ was 0.16 ±
652 0.03 and 0.18 ±0.06 in smoke PM_{1.0} and PM_{2.5}, respectively, which were almost one
653 order of magnitude larger than that in the ambient aerosol (Liu and Bei, 2016; Tao et
654 al., 2016). Tao et al. (2016) ever measured the ratio as a function of particle size
655 during NPF days in Shanghai, and a noticeable enrichment of aminiums for ultrafine
656 particles (<56 nm) was observed with WSA/NH₄⁺ over 0.2, highlighting the
657 competitive role for amines to ammonia in particle nucleation and initial growth of
658 the nuclei, the ratio was then decreased with the increasing particle size, and the final
659 increasing trend was found after ~ 1.0 μm, and average WSA/NH₄⁺ for ambient bulk
660 PM_{1.0} and PM_{2.5} were 3.2% and 3.5% , respectively.

661 **3.1.4 PAHs and Phenols**

662 Atmospheric PAHs are primarily the byproduct of incomplete combustion of
663 biomass and fossil fuels (Simcik et al., 1999; Galarneau, 2008). Due to their high
664 degree of bioaccumulation and carcinogenic or mutagenic effect, the sources and
665 environmental fate of the ubiquitous PAHs have been the subjects of extensive
666 studies (Santodonato, 1997; Kim et al., 2013). PAHs can involve in photochemical
667 reaction to form SOA, the process is influenced by gas-to-particle partition and
668 meteorological conditions. Moreover, oxidation may increase the toxicity of PAHs
669 (Arey and Atkinson, 2003; Wang et al., 2011). Biomass burning is one of the main
670 sources of gaseous and particulate PAHs, which even contributes to about half of
671 anthropogenic PAHs emissions in China (Xu et al., 2006; Zhang et al., 2011).
672 Burning conditions can significantly influence the emission of PAHs, under the
673 flaming phase in this study, PAHs contributed 0.46 wt.% of smoke PM_{2.5} and 0.28
674 wt.% of PM_{1.0}, over 60% of the total PAHs were associated to respiratory submicron
675 particles. The sum of EFs of 16 PAHs in smoke PM_{2.5} ranged from 1.81 to 8.30 mg

676 kg^{-1} , which were consistent with the values from literature (Dhammapala et al.,
677 2007a, b; Lee et al., 2005; Zhang et al., 2011). Hays et al. (2005) estimated total EFs
678 of 16 PAHs to be 3.3 mg Kg^{-1} in wheat straw burning $\text{PM}_{2.5}$. Korenaga et al. (2001)
679 measured PAHs EFs from rice straw burning to be 1.9 mg Kg^{-1} in particulate phase,
680 while the value from Jenkins et al. (1996) was 16 mg Kg^{-1} . Dhammapala et al.
681 (2007b) found negative linear response for biomass burning source PAHs emissions
682 to burning efficiency, and under flaming combustion, particulate total 16 PAHs EFs
683 were $2 \sim 4 \text{ mg Kg}^{-1}$. Zhang et al. (2011) simulated burning of rice, corn, and wheat
684 straws, the corresponded PAHs EFs were measured as 1.6, 0.9, and 0.7 mg Kg^{-1} in
685 fine smoke particles, respectively. Great uncertainties for PAHs EFs were evident
686 that relied on burning phase, fuel types, moisture content, and also measurement
687 techniques. Dhammapala et al. (2007a) also found laboratory simulation might
688 overestimate the emission factors of PAHs compared with field burnings. EFs for
689 individual PAHs were included in Table S8 and S9 (SI). The distribution of
690 particulate PAHs emission factors was presented in Fig. 3a. Of the particle bound
691 PAHs, 3~4-rings components were the primary ones, including Pyr, Ant, Ace, Flu,
692 Phe, and Chr. Concentration ratios of selected PAHs, namely diagnostic ratios, were
693 usually used to trace the source and make apportionment of specific pollutions
694 (Yunker et al., 2002; Simcik et al., 1999). In this work, average $\text{Ant}/(\text{Ant}+\text{Phe})$,
695 $\text{Flu}/(\text{Flu}+\text{Pyr})$, $\text{BaA}/(\text{BaA}+\text{Chr})$, and $\text{IP}/(\text{IP}+\text{BghiP})$ ratios of 5 types agricultural
696 residue burning smokes were 0.72, 0.36, 0.47, and 0.58, respectively. There was no
697 significant difference ($P < 0.05$ at 95% CI) of the ratios in $\text{PM}_{1.0}$ and $\text{PM}_{2.5}$. According
698 to previous work, $\text{Ant}/(\text{Ant}+\text{Phe})$ above 0.1 and $\text{BaA}/(\text{BaA}+\text{Chr})$ above 0.35 indicate
699 the dominance of combustion and pyrolytic sources, $\text{Flu}/(\text{Flu}+\text{Pyr})$ and $\text{IP}/(\text{IP}+\text{BghiP})$
700 ratios greater than 0.50 suggest coal or biomass burnings dominate (Simcik et al.,
701 1999; Yunker et al., 2002). However, validation of source apportionment using
702 specific diagnostic ratios should have its constraints, because of variations in source
703 strengths and atmospheric processing of PAHs (Arey and Atkinson, 2003; Galarneau,
704 2008).

705 From Table S10 (SI), PAHs in smoke particles were highly correlated with EC and

706 OC contents. PAHs primarily originate from pyrolysis of organic materials during
 707 combustion, and formation mechanisms of PAHs and soot are closely intertwined in
 708 flames. High-molecular-weight PAHs (>500 atomic mass unit) act as precursors of
 709 soot particles (Lima et al., 2005; Richter et al., 2000). Thus, PAHs with 3, 4, and 5
 710 rings accumulate and dominate in the emissions of biomass burning, as larger
 711 molecular weight PAHs tend to incorporate into soot particles. PAHs
 712 expulsion-accumulation in OC and EC fractions were analyzed by linear fitting of
 713 PAHs mass fractions and EC mass fractions in carbonaceous materials (EC+OC) in
 714 Fig. 3b. The partitions can be parameterized as Eq. (10):

$$715 \quad f_{\text{PAHs}} = \frac{m_{\text{PAHs}}}{m_{\text{OC}}+m_{\text{EC}}} = \beta_{\text{EC}} \times \frac{m_{\text{EC}}}{m_{\text{OC}}+m_{\text{EC}}} + \beta_{\text{OC}} \times \frac{m_{\text{OC}}}{m_{\text{OC}}+m_{\text{EC}}} = \beta_{\text{EC}} \times f_{\text{EC}} + \beta_{\text{OC}} \times f_{\text{OC}} \quad (10)$$

716 where f_{EC} and f_{OC} are the mass fraction of OC and EC in carbonaceous
 717 materials (EC+OC). β_{EC} and β_{OC} are expulsion-accumulation coefficients of PAHs in
 718 OC and BC. The coefficient of β_{EC} is 1.1×10^{-3} in smoke $\text{PM}_{1.0}$ and 1.9×10^{-3} in $\text{PM}_{2.5}$,
 719 the corresponded β_{OC} is 0.3×10^{-3} and 0.5×10^{-3} .

720 Phenols are the most common SOA precursor/product and organic pollutants in
 721 the atmosphere (Berndt and Böge, 2006; Schauer et al., 2001). Hydroxyl functional
 722 group and aromatic benzene ring make phenols a paradigm in heterogeneous
 723 reaction upon photo oxidation research and aqueous phase reaction research. Phenols
 724 are also ROS (reactive oxidized species) precursors that present health hazard (Bruce
 725 et al., 1987). Phenol and substituted phenols are thermal products of lignin pyrolysis
 726 during biomass burning (Dhammapala et al., 2007a), and the most abundant
 727 methoxyphenols can be markers of biomass burning sources (Urban et al., 2016).
 728 The five measured phenols contributed 3.0 wt.% and 2.5 wt.% of $\text{PM}_{2.5}$ and $\text{PM}_{1.0}$.
 729 2, 6-dimethoxyphenol was the major one of the measured phenols. Mass fraction of
 730 phenols was about 7~9 times of PAHs in smoke aerosols. EFs for the sum phenols
 731 were 9.7 ~ 41.5 and 7.7 and 23.5 mg Kg^{-1} for smoke $\text{PM}_{2.5}$ and $\text{PM}_{1.0}$, respectively.
 732 Dhammapala et al. (2007a) estimated particulate methoxyphenols emissions to be 35
 733 $\pm 24 \text{ mg Kg}^{-1}$ for wheat straw burning, while Hays et al. (2005) measured the same
 734 compounds to be 6.8 mg Kg^{-1} . Carbonaceous materials like PAHs and Phenols or

735 aromatic and phenolic deviates are the main chromophores in the atmosphere, and
736 the considerable fractions of PAHs and Phenols justify biomass burning as a
737 significant source of brown carbon (Laskin et al., 2015), study has proved ~ 50% of
738 the light absorption in the solvent-extractable fraction of smoke aerosol can be
739 attributed to these strong BrC chromophores (Lin et al., 2016).

740 **3.1.5 Inorganic components**

741 From Fig. 2, smoke particles consisted of approximately 24 wt.% water soluble
742 inorganics (WSI), and the inorganic salts resided more in submicron particles. Great
743 amount of inorganics enable smoke particles to be efficient CCN, and the distinct
744 optical scattering characters of the inorganic fractions may neutralize the warming
745 effect of brown carbon for smoke aerosol, otherwise, inorganics coating or mixing
746 will enhance light absorbing of BC. K^+ , NH_4^+ , Cl^- , and SO_4^{2-} were the principle
747 inorganic ions. Particulate enriched K^+ together with levoglucosan are treated as tracer
748 of pyrogenic source (Andreae et al., 1998). And specific mass ratio of K^+/OC or
749 K^+/EC will help make source apportionment of particulate pollutants with PMF
750 (Positive Matrix Factorization) and PFA (Principle Balance Analysis) models (Lee et
751 al., 2015). K^+/OC in smoke particles ranged from 0.11 to 0.25 with average value of
752 0.17 in $PM_{1.0}$ and 0.14 in $PM_{2.5}$, which were similar to those reported for the
753 Savannah burning and agricultural waste burning emissions in India and China
754 (Echalar et al., 1995; Ram and Sarin, 2011; Li et al., 2015). However, OC represents
755 large uncertainty arise from degree of oxidization and burning condition, K^+/EC is
756 more practical parameter to distinguish the pyrogenic pollutants in ambient study. To
757 smoke particle emitted from flaming fires, K^+/EC was 0.58 ± 0.24 in $PM_{1.0}$ and 0.53
758 ± 0.18 in $PM_{2.5}$. Cl^- was the main anion to balance the charge of WSI in smoke
759 particles. Mean charge ratio of $Cl^- : K^+$ was 1.46 and 1.49 in $PM_{1.0}$ and $PM_{2.5}$,
760 implicating surplus chloride will associate with other cations. With atmospheric
761 aging, the Cl^-/K^+ ratio will decrease as chloride being replaced by secondary sulfate
762 and nitrate (Li et al., 2015; Li et al., 2003). Equivalent charge ratio of primary

763 cations ($\text{NH}_4^+ + \text{K}^+$) to primary anions ($\text{SO}_4^{2-} + \text{Cl}^-$) was 1.05 in $\text{PM}_{1.0}$ and 1.01 in
764 $\text{PM}_{2.5}$ on average, and charge ratios of total cations to anions ($R_{C/A}$) was 1.09 and
765 1.07 in $\text{PM}_{1.0}$ and $\text{PM}_{2.5}$. $R_{C/A}$ was used to indicate the neutralizing level of
766 particulate matters in many studies. $R_{C/A} \geq 1$ indicates most of the acids can be
767 neutralized, while $R_{C/A} < 1$ means atmospheric ammonia is deficient and the aerosol is
768 acidic (Adams et al., 1999; He et al., 2011a; Kong et al., 2014). In ambient
769 environment, acidic aerosol was prevailing urban pollutants in many cities from field
770 investigation (He et al., 2011a; Kong et al., 2014). Acidic aerosols can increase the
771 risks to human health and affect the atmospheric chemistry by activating hazardous
772 materials and promoting the solubility of particulate iron and phosphorus (Amdur
773 and Chen, 1989; Meskhidze, 2005). The emission and transport of biomass burning
774 particles may neutralize the acidity of ambient particles. However, only limited WSI
775 were brought into in the analytical system, it is not really to tell the acidity or base of
776 smoke particles, considering the existence of massive organic acids and ammoniums.

777 Trace mineral elements attracted great attention for the role as catalyst in
778 atmospheric heterogeneous reaction and health cares (Davidson et al., 2005;
779 Dentener et al., 1996). Wet/dry deposition of particles during long range transport
780 will affect the ecological balance by releasing mineral elements (Jickells et al., 2005).
781 Dust storm, weathering, and industrial process are the main sources of particulate
782 metals, and incineration can also produce a lot of mineral elements (Moreno et al.,
783 2013). However, the emissions of trace metals from biomass burning are highly
784 uncertain (Li et al., 2007; Zhang et al., 2012), the great influence from local soil
785 environment and soil heavy metal pollution will certainly affect the metal content in
786 biomass fuel and smoke particle. In this study, THM resided more in $\text{PM}_{2.5}$ than in
787 $\text{PM}_{1.0}$. Smoke $\text{PM}_{2.5}$ consisted of 6.7 wt.% THM on average, $\text{PM}_{1.0}$ comprised 4.1
788 wt.% THM. Average EFs of THM in $\text{PM}_{2.5}$ and $\text{PM}_{1.0}$ were 0.056 g kg^{-1} and 0.028 g
789 kg^{-1} in this work, of which Al contributed over 90 wt.%, in line with result from
790 domestic burning of wood and field investigation of crop straw burning (Li et al.,
791 2007; Zhang et al., 2012). Smoke particles from wheat, rice, and corn straws
792 contained more mineral elements than that from cotton and soybean residues

793 combustion. Regardless the difference in biomass fuels, the result may imply that
794 soil heavy metal pollution is heavier in the East China than that in Xinjiang in the
795 West North of China (Wei and Yang, 2010).

796 **3.2 Size, morphology, and mixing state of smoke particles**

797 Fresh smoke particles exhibited unimodal size distribution within 500 nm (Fig. S3,
798 SI), and previous chamber study has also confirmed that agricultural fire produces
799 large amount of ultrafine particles, implying the great potential role to act as CCN
800 and more profound threat to human health (Araujo et al., 2008; Delfino et al., 2005;
801 Zhang et al., 2011). However, the role of particles in the atmospheric process and
802 health hazard depends not only size, but also morphology and chemical mixing
803 states (Dusek et al., 2006; Kennedy, 2007; Mikhailov et al., 2006; Schlesinger, 1985).
804 From TEM images in Fig. 4, agricultural straw burning aerosols comprised a broad
805 class of morphological and chemically heterogeneous particles. Non-uniformly
806 internal mixing of the agglomerates was noticeable, including the major
807 carbonaceous particles and a considerable amount of inorganic salt particles, which
808 was consistent with previous particulate chemical analysis. KCl particles containing
809 minor sulfate or nitrate were the primary inorganic particles, which presented crystal
810 or amorphous state from X-ray diffraction analysis (Fig. 4 a, b, c). And
811 potassium-bearing particles have been used as a tracer of ambient biomass burning
812 pollutants. Fly ash particles were arresting due to visible morphology difference and
813 mineral chemical composition (Fig. 4 d, e, f). Fly ash particles were more compact
814 and rich in mineral elements like Ca, Si, Fe, Al, Mn, and Cr. Besides, these particles
815 had larger size, statistical average diameter of fly ash particles obtained from bulk
816 analysis was $2.2 \pm 1.6 \mu\text{m}$. The result also proved heavy metals resided more in
817 $\text{PM}_{2.5}$ than $\text{PM}_{1.0}$. Fly ashes are by products of incineration process (Buha et al.,
818 2014), including coagulation of fuel issue debris, condensation of evaporated
819 mineral metal from biomass fuels or adhered dirt at different burning phase. These
820 fly ashes coated by or agglomerated with carbonaceous materials were like mash of

821 mineral without clear lattice. Tar ball as a specific form of brown carbon and soot
822 were representative particles of biomass burning aerosol (Wilson et al., 2013;
823 Chakrabarty et al., 2010; Tóth et al., 2013). From Fig. 4 g, chain-like soot particles
824 were coagulated with tar ball. Soot particles were agglomerates of small roughly
825 spherical elementary carbonaceous particles, these chemical consistent particles were
826 within 20~30 nm, and high-resolution TEM showed the soot spheres consisted of
827 concentrically wrapped graphitic layers, while monomeric tar balls possessed
828 disordered microstructure. Tar balls and soot corresponded to different stages in the
829 aging of organic particles; tar balls abundant in fresh or slightly aged biomass smoke
830 are formed by gas-to-particle conversion of high-molecular weight organic species
831 or from aged primary tar droplets upon biomass burning. Soot represents further
832 aged carbon-bearing particles, formed from the pyrolysis of lignin, cellulose, or tar
833 balls (Pósfai, 2004; Tóth et al., 2013). The botryoid aggregates in Fig. 4 g can be
834 viewed as transformation of tar ball to soot. Tar ball and soot were also internal
835 mixed with inorganic salt including sulfate and nitrate (Fig. 4 g, h, i), which made
836 the physiochemical properties of BC even complicated, as study has confirmed
837 inorganic sulfate mixing will enhance light absorption and hygroscopicity of BC
838 (Zhang et al., 2008b). Dark-ring like shell of tar ball (Fig. 4 g, h) and spot-like
839 particles adhered to the surface of tar ball (Fig. 4 i) were K-rich materials. And size
840 of soot particles was mainly within 200 nm, while tar ball and other carbonaceous
841 particles can be over one micrometer.

842 **3.3 Open burning emissions**

843 **3.3.1 Crop straw production**

844 The agricultural straw productions were calculated and geographically displayed in
845 Fig. 5 a-c. Totally 647.3 Tg agricultural straws were produced in 2012 and dispersed
846 mainly in the North and Northeast of China. The distributions of the straws clearly
847 correspond to the distinct planting regions that are divided by Qinling
848 Mountain-Huaihe River line and the Yangtze River. Rice is primarily planted in the

849 south of Qinling Mountain-Huaihe River line, only 10 % rice (single cropping rice
850 dominate) is planted in Heilongjiang, Jilin, and Liaoning province, while wheat and
851 corn are grew mostly in the north of the Yangtze River. Over 90 % of the wheat
852 planted in China is winter wheat that gets ripe in summer, and more than 80 % rice
853 including middle and late rice grows mature in autumn. Summer harvest contributed
854 about 25 % of the agricultural straw production, which solely consists of rice and
855 wheat straws in this period and distributes uniformly in the central and east of China.
856 493.9 Tg crop straws were produced mainly from corn and rice harvesting in autumn.
857 Soybean and cotton straws account for about 8.6 % of autumn straw production that
858 were primarily produced in Heilongjiang and Xinjiang province.

859 **3.3.2 Open burning rate**

860 The five scenarios of field burning rates and regional AIP ($\frac{I_{k,y}}{AI_{k,y}}$) in the year of
861 2000, 2006, and 2012 were listed in Table 4 and statistically analyzed in Fig. 6. A
862 significant difference ($P < 0.05$ at 95% CI) of regional burning rates among the
863 versions was observed, and the rates from NDRC report were generally higher. For
864 convenience, six zones were classified by geographic divisions and economic areas
865 in China, including the North Plain of China (NPC: Anhui, Shandong, Hebei, Shanxi,
866 Tianjin, Beijing), the Central of China (CC: Hunan, Henan, Hubei), the Yangtze
867 River Delta (YRD: Zhejiang, Jiangsu, Shanghai), the Northeast of China (NC:
868 Heilongjiang, Liaoning, Jilin), the Pan-Pearl River Delta (PRD: Hainan, Guangdong,
869 Fujian, Guangxi, Guizhou, Sichuan, Yunnan, Jiangxi), the West of China (WC:
870 Shanxi, Chongqing, Xinjiang, Qinghai, Ningxia, Tibet, Inner Mongolia, Gansu).
871 And the bulk-weighted burning rates that averaged from BAU, EM, and NDRC
872 versions for the six zones were 22.3 % \pm 3.1 %, 21.1 % \pm 3.3 %, 28.4 % \pm 6.2 %,
873 23.3 % \pm 9.2 %, 21.4 % \pm 6.5 %, and 14.2 % \pm 8.0 %, respectively. It was obvious
874 that agricultural field burning was most serious in the Yangtze River Delta,
875 especially in the Zhejiang province. The nationwide field burning rate was 21.4 %, 16.3 %, 26.0 %, 14.9 %, and 26.8 % for BAU-I, BAU-II, EM-I, EM-II, and NDRC,

877 respectively, which were comparable with the document values (Daize, 2000; Wei et
878 al., 2004; Zhang et al., 2008a).

879 **3.3.3 Agricultural open burning emissions**

880 PM_{2.5} emissions from agricultural field burnings based on BAU, EM, and NDRC
881 versions were calculated and geographically presented in Fig. 7 (emissions of
882 detailed individual species in SI). A similar spatial character of regional emission
883 distribution was observed for BAU, EM, and NDRC versions, most emissions were
884 allocated in the North Plain and the Central of China, where the primary agricultural
885 regions locate, echoing the agricultural fire sites in Fig. S2 (SI). Although filed
886 burning rates were higher in the Yangtze River Delta, the crop residue productions in
887 this zone were much less, which only contributed 4.3 % of the national straw
888 productions. Take NDRC as the basis, BAU and EM scenarios all underestimated the
889 emissions in the Northeast of China, especially in Heilongjiang.

890 The temporal distributions of field burning emissions also echoed the crop residue
891 productions and the agricultural fire sites in summer and autumn harvest. Apart from
892 Henan and Tibet where the main crop straws were produced in summertime, more
893 pollutants were emitted in autumn harvest period to the rest place, which has been
894 confirmed by many studies (He et al., 2011; Wang and Zhang, 2008). And the large
895 scale filed burning emissions in autumn exhibited great influence on the haze
896 formation and visibility degradation in the North and East of China (Leng et al.,
897 2014; Shi et al., 2014), Huang et al. (2012a) has identified biomass burning together
898 with secondary inorganic aerosol (SIA) and dust pollution as three typical haze types
899 in Shanghai. In summertime, filed burning emissions concentrated in the North Plain,
900 the Central, and the South regions. While in autumn, the emissions became more
901 ubiquitous and serious in the Northeast of China.

902 Nationwide emission inventories and flux concentrations were graphically
903 displayed in Fig. 8 and tabular presented in Table 5. The total PM_{2.5} emission from
904 agricultural field burnings was 738.36-1241.69 Gg in 2012, and rice, corn, and

905 wheat straw burnings made up 93.5% ~ 95.6% of the total emissions. The largest
906 quantities of PM_{2.5} emissions were emitted from Heilongjiang, Shandong, Henan,
907 Jilin, Jiangsu, Anhui and Hebei, distinct difference in the emissions from various
908 scenarios were observed, especially for Heilongjiang province which contributed
909 5.5 % (55.4 Gg) of PM_{2.5} emissions under BAU-II scenarios, while the figure was
910 22.9 % (231.0 Gg) under EM-I scenarios. Annual emissions of PM_{1.0}, OC, and EC
911 was 661.81-1111.90, 318.84-533.19, and 98.06-164.97 Gg, respectively, which were
912 comparable with the precious studies (Cao et al., 2006, 2011; Wang et al., 2012). Qin
913 and Xie (2011, 2012) developed national carbonaceous aerosol emission inventories
914 from biomass open burning for multi-years with dynamic burning activity, they
915 believed BC and OC emissions followed an exponential growth from 14.03 and
916 57.37 Gg in 1990 to 116.58 and 476.77 Gg in 2009. Cao et al. (2006, 2011)
917 calculated smoke aerosol emissions from biomass burning in China for 2000 and
918 2007 using the same activity data from BAU-I scenarios, national OC and EC
919 emissions were reported to be 425.9 and 103.0 Gg in 2000, however, no evident
920 changes were found for the emissions in 2007, which were assessed to be 433.0 and
921 104.0 Gg. Huang et al. (2012b) estimated crop burning in the fields with unified EFs
922 and burning rate (~6.6%) for all kinds of crops across China in 2006, the estimated
923 annual agricultural fire emissions were about 270, 100, and 30 Gg for PM_{2.5}, OC,
924 and BC, respectively. In present work, agricultural fire PM_{2.5} emissions in 2012 were
925 allocated into six zones, average contribution in percentage for each zone was
926 compared: NPC (23.1%) ≥ NC (21.6%) > PRD (18.4%) ≥ CC (18.2%) > WC
927 (9.8%) > YRD (8.8%). Furtherly, contribution for summertime emissions was: NPC
928 (35.5%) > CC (28.8%) ≥ PRD (21.1%) > YRD (9.1%) > WC (5.4%) > NC (0.1%),
929 and for autumn harvest emissions: NC (27.8%) > NPC (19.6%) > PRD (17.6%) >
930 CC (15.1%) > WC (11.1%) > YRD (8.8%). It was obviously that the North Plain
931 experienced extensive crop fire emissions during the whole harvest periods, where
932 PM_{2.5}, PM_{1.0}, OC, and BC emissions in 2012 were 233.6, 209.8, 102.3, and 29.4 Gg
933 on average. Liu et al. (2015) developed emission inventories from agricultural fires
934 in the North Plain based on MODIS fire radiative power, emission for PM_{2.5}, OC,

935 and BC in 2012 was reported to be 102.3, 37.4, and 13.0 Gg, respectively. However,
936 EFs were also treated as unified values (e.g., Crop burning EFs for PM_{2.5}, OC, and
937 BC was 6.3, 2.3, and 0.8 g Kg⁻¹) in the work of Liu et al. (2015) that was cited
938 directly from Akagi et al. (2011) without considering fuel type dependence of EFs.
939 Zhao et al. (2012) established comprehensive anthropogenic emission inventories for
940 Huabei Region including the North Plain, Inner Mongolia, and Liaoning province,
941 all crop straws were assumed to be burnt in the field, resulting in much more
942 emissions of 446 Gg OC and 160 Gg BC in 2003. A specific temporal pattern for
943 agricultural fire emissions was observed in the Northeast of China (Heilongjiang,
944 Liaoning, and Jilin), where the open burning were mainly occurred in autumn
945 harvest to produce great amount of pollutants (217.5 Gg PM_{2.5}, 89.4 Gg OC, and
946 29.7 Gg EC), while emissions in the summertime can be neglected.

947 In 2012, 20-25 % of national emissions were released from summertime field
948 burnings, that was 226.0 Gg PM_{2.5}, 205.2 Gg PM_{1.0}, 105.9 Gg OC, 28.4 Gg EC, 6.8
949 Gg WSOA, 1.0 Gg WSA, 0.1 Gg PAHs, 0.9 Gg phenols, and 2.1 Gg THM on
950 average. The corresponded values for autumn harvest were 781.6, 697.9, 327.3,
951 106.0, 18.4, 4.8, 0.4, 1.9, and 6.6 Gg, respectively. Integrated smoke OC/EC was 3.7
952 from national summertime emission and 3.1 from autumn harvest emission,
953 regarding to different locations, integrated OC/EC in the North Plain was 4.1 in
954 summertime emission and 3.2 in autumn harvest, while OC/EC in the Central of
955 China was 3.1 for both summer and autumn harvest emissions, implying
956 temporal-spatial characters of agricultural field fires exhibit potential influence on
957 composition of smoke emissions and its related physiochemical properties. Zhang et
958 al. (2011) estimated particulate PAHs emissions from three types of crop residues to
959 be 0.46 Gg in 2003. Xu et al. (2006) counted PAHs from all straws with the
960 assumption that burning rates to be unit, and they calculated 5-10 Gg PAHs
961 emissions in 2003, which was ten times of our result.

962 The nationwide flux concentration of smoke PM_{2.5} was 0.7-1.0 µg m⁻³ d⁻¹ in
963 summer harvest and 1.4-3.5 µg m⁻³ d⁻¹ in autumn harvest, while average annual flux
964 concentrations for OC and EC were 0.80 and 0.25 µg m⁻³ d⁻¹. Saikawa et al. (2009)

965 assessed the annual concentrations of OC and BC from biomass burning primary
966 emission in China using global models of chemical transport (MOZART-2) to be 1.8
967 and $0.35\mu\text{g m}^{-3}$. The most polluted areas were Anhui, Henan, Shandong, Jiangsu,
968 Liaoning, and Hunan.

969 **3.3.4 Uncertainties of the emissions**

970 The fuzziness and uncertainties of major pollutants emissions from fuel combustion
971 in China came from the uncertainties in specific-source emission factors and
972 effective consumption of bio- or fossil fuel. Frey et al. analyzed uncertainties in
973 emission factors and emissions of air toxic pollutants and technology dependent
974 coal-fire power plants via bootstrap simulation method (Frey and Zhao, 2004; Frey
975 and Zheng, 2002). Zhao et al. estimated uncertainties in national anthropogenic
976 pollutants emissions based on Monte Carlo simulation, and they believed activity
977 rates (e.g. fuel consumption) are not the main source of emissions uncertainties at the
978 national level (Zhao et al., 2011; Zhao et al., 2012). The uncertainties in emission
979 inventory can also be estimated by comparing different emission inventories for the
980 same region and period (Ma and Van Aardenne, 2004).

981 In this study, we investigated the uncertainties of multi-pollutants emissions for
982 agricultural residue open burning using Monte Carlo Simulation. Detailed
983 methodology was referred to Qin and Xie (2011). We followed the assumption: a
984 normal distribution with coefficient of variation (CV) of 30% for the official
985 statistics (e.g., crop production and GDP economic data obtained from Statistic
986 Yearbooks, field burning rates for agricultural straw derived from NDRC report,
987 etc.), a normal distribution with 50% CV for open burning rates from literature
988 (BAU-I and BAU-II), and a uniform distribution with $\pm 30\%$ deviation for the rest
989 activity data (crop-to-residue ratio, dry matter fraction, and burning efficiency).
990 Regarding the emission factors, Bond et al. (2004) assumed that most particulate
991 EFs followed lognormal distributions with CV of $\pm 50\%$ for domestic EFs, and of \pm
992 150% for EFs obtained from foreign studies. Here, we applied the CV of smoke

993 EFs as we measured ones, which were chemical species and fuel type dependent.
994 With randomly selected values within the respective probability density functions
995 (PDFs) of EFs and activity data for each biomass type, Monte Carlo simulation was
996 implemented for 10,000 times, and the uncertainties in national yearly
997 multi-pollutants emissions at 95% CI were obtained for all the 5 versions.
998 Afterwards, uncertainties for the average emission inventories were assessed using
999 the propagation of uncertainty calculation that suggested by IPCC (1997) (method
1000 in SI), and all the emission uncertainties were presented in percentage in Table 6.
1001 Emissions for water soluble aminiums and organic acids had the vast uncertainties,
1002 due to their large deviation in EFs compared with other smoke species. Besides,
1003 emissions of BAU versions were more accurate than EM versions, because of more
1004 uncertainty addition in the burning rates conversion using economic data for EM
1005 versions. Otherwise, burning rates derived from NDRC report were assumed to
1006 have less uncertainty, resulting in the least uncertainties in smoke emission
1007 assessments. On average of all the 5 versions, mean, 2.5th percentile, and 97.5th
1008 percentile values for smoke PM_{2.5} emissions in 2012 were 1005.7, 758.3, and
1009 1344.6 Gg, respectively. As to OC emissions, mean, 2.5th percentile, and 97.5th
1010 percentile values were 432.4, 327.8, and 576.4 Gg, the figure for EC was 134.2,
1011 100.9, and 187.9 Gg. Therefore, the overall propagation of uncertainties for smoke
1012 PM_{2.5}, OC, and EC at 95% CI was (-24.6%, 33.7%), (-24.4%, 33.5%), and (-24.2%,
1013 33.3%), respectively. The uncertainties for OC and EC emissions were much less
1014 than the work of Qin and Xie (2011), in which emission and uncertainties were
1015 266.7 Gg (-55.9%, 96.1%) for OC and 66.9 Gg (-53.9%, 92.6%) for EC in 2005.

1016 **3.4 Health and health-related economic impacts**

1017 **3.4.1 Carcinogenic risk**

1018 Calculated CR_{SPM} for smoke PM_{2.5} from wheat, corn, rice, cotton, and soybean
1019 straw burning were 5.3×10^{-6} , 3.8×10^{-6} , 2.6×10^{-6} , 0.7×10^{-6} , and 1.3×10^{-6} per $\mu\text{g m}^{-3}$,
1020 respectively. And the corresponded one in million PEL was 0.2, 0.3, 0.4, 1.4, and 0.8

1021 $\mu\text{g m}^{-3}$. Wu et al. (2009) ever assessed unit risk of wood and fuel burning particles
1022 using metals merely, the results were 3.2×10^{-6} and 1.5×10^{-6} per $\mu\text{g m}^{-3}$, which were
1023 close to that in our study. In actual application, PEL of smoke particles should be
1024 bulk mass concentration of mixed aerosols.

1025 It was noticeable that apart from Tibet and Qinghai, the flux concentration of
1026 smoke $\text{PM}_{2.5}$ among all the five emission versions in other regions far surpassed the
1027 PEL, especially the North Plain and the Central of China, exhibiting great potential
1028 inhalable cancer risk. For the health care, emission flux concentration should be
1029 constrained within the PEL of crop straw burning aerosol. Thus the critical field
1030 burning rates can be derived to ensure risk aversion following Eq. (11):

$$1031 \quad R_k \leq \frac{10^{-6} \times S_k \times h \times T_k}{\sum_j \sum_i P_{t,k,i} \times r_i \times H_{t,k,i} \times D_i \times f_i \times EF_{i,j} \times CRF_i} \quad (11)$$

1032 The conservative values of regional field burning rates from Eq. (11) were named
1033 as Carcinogenic Risk Control scenarios (CRC) and listed in Table S11 (SI), which
1034 would be instructive in emission control. Under CRC, national crop straw field
1035 burning rate was less than 3%, emissions of $\text{PM}_{2.5}$ were geographically presented in
1036 Fig. S4 (SI), and 146.3 Gg yr^{-1} smoke $\text{PM}_{2.5}$ should be released at largest in China,
1037 the corresponded annual flux concentration of $\text{PM}_{2.5}$ was within $0.3 \mu\text{g m}^{-3} \text{ d}^{-1}$
1038 (detailed emission inventories under CRC version see in SI).

1039 **3.4.2 Health impacts**

1040 Regional health impacts from acute exposure of agricultural residue burning aerosol
1041 were assessed using average daily flux concentrations of smoke $\text{PM}_{2.5}$, the result was
1042 tabulated in Table S12 (SI). The impacts from smoke $\text{PM}_{2.5}$ exposure were severest
1043 in Jiangsu, Shandong, and Henan province, where annual premature mortality was
1044 over one thousand. Overall, China suffered from 7836 (95% CI: 3232, 12362)
1045 premature death, 31181 (95% CI: 21145, 40881) respiratory hospital admissions,
1046 29520 (95% CI: 12873, 45602) cardiovascular hospital admissions, and 7267237 (95%
1047 CI: 2961487, 1130784) chronic bronchitis related to agricultural fire smoke in 2012
1048 from Table 7. According to national health statistical reports (NHFPC, 2013), the

1049 hospital admission due to respiratory and cardiovascular disease was 5071523 in
1050 China in 2012, and smoke PM_{2.5} exposure might contribute ~1.2% of the hospital
1051 admissions from this study. Saikawa et al. (2009) ever reported 70000 premature
1052 deaths in China and an additional 30000 deaths globally due to OC, EC, and sulfate
1053 exposure that were primarily emitted from biofuel combustion in China in 2000,
1054 however, the results should be overestimated not only in the exaggerated pollutant
1055 emissions but also in the iterative operations of respective species induced mortality,
1056 besides, the exposure-response coefficient β and incidence rate he applied from Pope
1057 et al. (2002) and WHO (2000) were higher than the practical values from local
1058 research (Cao et al., 2012; Chen et al., 2011; Hou et al., 2012). From Table 7, under
1059 CRC version, over 92 % mortality and morbidity can be avoided.

1060 **3.4.3 Health-related economic losses**

1061 Health-related total economic losses from straw open burning smoke PM_{2.5} exposure
1062 were assessed to be 8822.4 (95 % CI: 3574.4, 13034.2) million US\$ on average from
1063 Table 8, accounting for 0.1% of the total GDP in 2012, and detailed regional
1064 economic losses were listed in Table S13. Economic losses from premature death
1065 contributed about 17% of total losses, and loss from chronic bronchitis dominated.
1066 Hou et al. (2012) ever estimated 106.5 billion US\$ lost due to ambient PM₁₀
1067 exposure in China in 2009; even a severe haze episode (PM_{2.5} be focused on) in
1068 January 2013 may cause 690 premature death and 253.8 million US\$ loss in Beijing,
1069 and source-specification analysis stressed the emission from biomass burning (Yang
1070 et al., 2015; Gao et al., 2015). It was obvious that smoke PM_{2.5} contributed a
1071 noticeable damage to public health and social welfare. According to CRC version
1072 estimation, the carcinogenic risk control policy can save over 92 % of the economic
1073 loss.

1074 **4 Conclusion**

1075 Detailed chemical compositions of smoke aerosol from five major agricultural

1076 straws burning were characterized using an aerosol chamber system. And
1077 corresponded emission factors for particulate OC-EC, WSI, WSOA, WSA, PAHs,
1078 Phenols, and THM in smoke PM_{2.5} and PM_{1.0} were established.

1079 Permissible exposure limits (PEL) of the smoke particles were assessed for
1080 carcinogenic risk concern based on selected hazard pollutants including PAHs and
1081 THM in smoke PM_{2.5}. Daily exposure concentration should be constrained within
1082 0.2, 0.3, 0.4, 1.4, and 0.8 μg m⁻³ for wheat, corn, rice, cotton, and soybean straw,
1083 respectively.

1084 Emission inventories of primary particulate pollutants from agricultural field
1085 burning in 2012 were estimated based on BAU-I, BAU-II, EM-I, EM-II, and NDRC
1086 scenarios, which were further allocated into different regions at summer and autumn
1087 open burning periods. The estimated total emissions were 1005.7 Gg PM_{2.5} (95%CI:
1088 -24.6% , 33.7%), 901.4 Gg PM_{1.0} (95%CI: -24.4%, 33.5%), 432.4 Gg OC (95%CI:
1089 -24.2%, 33.5%), 134.2 Gg EC (95%CI: -24.8%, 34.0%), 249.8 Gg WSI (95%CI:
1090 -25.4%, 34.9%), 25.1 Gg WSOA (95%CI: -33.3%, 41.4%), 5.8 Gg WSA (95%CI:
1091 -30.1%, 38.5%), 8.7 Gg THM (95%CI: -26.6%, 35.6%), 0.5 Gg PAHs (95%CI:
1092 -26.0%, 34.9%), and 2.7 Gg Phenols (95%CI: -26.1%, 35.1%), respectively. The
1093 spatial and temporal distributions of the five versions have similar characters that
1094 echo to the agricultural fires sites from satellite remote sensing. Less than 25 % of
1095 the emissions were released from summer field burnings that were mainly
1096 contributed by the North Plain and the Central of China. Flux concentrations of
1097 annual smoke PM_{2.5} that were calculated using box-model method based on five
1098 versions all exceed the PEL. From assessment of health impacts and health-related
1099 economic losses due to smoke PM_{2.5} short-term exposure, China suffered from 7836
1100 (95%CI: 3232, 12362) premature mortality and 7267237 (95% CI: 2961487,
1101 1130784) chronic bronchitis in 2012, which led to 8822.4 (95%CI: 3574.4, 13034.2)
1102 million US\$, or 0.1 % of the total GDP losses.

1103 Percentage of open burned crop straws at post-harvest period should cut down to
1104 less than 3% to ensure risk aversion from carcinogenicity, especially the North Plain
1105 and the Northeast, where the emissions should decrease at least by 94% to meet the

1106 PEL. And by applying such emission control policy, over 92% of the mortality and
1107 morbidity attributed to agricultural fire smoke PM_{2.5} can be avoided in China.

1108 **Supplementary material related to this article is available online at:**

1109 *Acknowledgment.* This work is supported by National Natural Science Foundation of
1110 China (No. 21190053, 21177025), Cyrus Tang Foundation (No. CTF-FD2014001),
1111 Shanghai Science and Technology Commission of Shanghai Municipality (No.
1112 13XD1400700, 12DJ1400100), Priority fields for Ph.D. Programs Foundation of
1113 Ministry of Education of China (No. 20110071130003) and Strategic Priority
1114 Research Program of the Chinese Academy of Sciences (Grant No. XDB05010200).

1115

References:

- 1116 Ackerman, A. S.: Reduction of Tropical Cloudiness by Soot, *Science*, 5468, 1042-1047, 2000.
- 1117 Adams, P. J., Seinfeld, J. H. and Koch, D. M.: Global concentrations of tropospheric sulfate, nitrate,
1118 and ammonium aerosol simulated in a general circulation model, *J. Geophys Res*, D11:13791-13823,
1119 1999.
- 1120 Akagi, S. K., Yokelson, R. J., Wiedinmyer, C., Alvarado, M. J., Reid, J. S., Karl, T., Crouse, J. D. and
1121 Wennberg, P. O.: Emission factors for open and domestic biomass burning for use in atmospheric
1122 models, *Atmos Chem. Phys.*, 9, 4039-4072, 2011.
- 1123 Amdur, M. O. and Chen, L. C.: Furnace-Generated Acid Aerosols: Speciation and Pulmonary Effects,
1124 *Environ. Health Persp.*, 79, 147-150, 1989.
- 1125 Andreae, M. O. and Gelencsér, A.: Black carbon or brown carbon? The nature of light-absorbing
1126 carbonaceous aerosols, *Atmos Chem. Phys.*, 10, 3131-3148, 2006.
- 1127 Andreae, M. O. and Merlet, P.: Emission of trace gases and aerosols from biomass burning, *Global*
1128 *Biogeochem Cy.*, 4, 955-966, 2001.
- 1129 Andreae, M. O., Andreae, T. W., Annegarn, H., Beer, J., Cachier, H., le Canut, P., Elbert, W.,
1130 Maenhaut, W., Salma, I., Wienhold, F. G., and Zenke, T. :, Airborne studies of aerosol emissions from
1131 savanna fires in southern Africa: 2. Aerosol chemical composition, *J. Geophys Res.*, D24, 32119-32128,
1132 1998.
- 1133 Araujo, J. A., Barajas, B., Kleinman, M., Wang, X., Bennett, B. J., Gong, K. W. Navab, M., Harkema,
1134 J., Sioutas, C., Lulis, A. J., and Nel, A. E.: Ambient particulate pollutants in the ultrafine range promote
1135 early atherosclerosis and systemic oxidative stress, *Circ Res.*, 5, 589-596, 2008.
- 1136 Arey, J. and Atkinson, R.: Photochemical reactions of PAHs in the atmosphere, PAHs: An
1137 *Ecotoxicological Persp.*, 47- 63, doi: 10.1002/0470867132.ch4, 2003.
- 1138 Arora, P. and Jain, S.: Estimation of Organic and Elemental Carbon Emitted from Wood Burning in
1139 Traditional and Improved Cookstoves Using Controlled Cooking Test, *Environ. Sci. Technol.*, 6,
1140 3958-3965, 2015.
- 1141 Aunan, K. and Pan, X.: Exposure-response functions for health effects of ambient air pollution
1142 applicable for China-a meta-analysis, *Sci. Total Environ.*, 329, 3-16, 2004.
- 1143 Aurell, J., Gullett, B. K. and Tabor, D.: Emissions from southeastern U.S. Grasslands and pine
1144 savannas: Comparison of aerial and ground field measurements with laboratory burns, *Atmos. Environ.*,
1145 111, 170-178, 2015.

1146 Bell, R. W. and Hipfner, J. C.: Airborne Hexavalent Chromium in Southwestern Ontario, *J. Air Waste*
1147 *Manage*, 8, 905-910, 1997.

1148 Berndt, T. and Böge, O.: Formation of phenol and carbonyls from the atmospheric reaction of OH
1149 radicals with benzene, *Phys. Chem. Chem. Phys.*, 10, 1205-1214, doi:10.1039/B514148F, 2006.

1150 Bølling, A. K., Pagels, J., Yttri, K. E., Barregard, L., Sallsten, G., Schwarze, P. E. and Boman, C.:
1151 Health effects of residential wood smoke particles: the importance of combustion conditions and
1152 physicochemical particle properties, *Part. Fibre Toxicol.*, 29, doi:10.1186/1743-8977-6-29, 2009.

1153 Bond, T. C.: A technology-based global inventory of black and organic carbon emissions from
1154 combustion, *J. Geophys Res.*, 109, D14203, doi:10.1029/2003JD003697, 2004.

1155 Bond, T. C., Doherty, S. J., Fahey, D. W., Forster, P. M., Berntsen, T., DeAngelo, B. J. Flanner, M. G.,
1156 Ghan, S., Kärcher, B., Koch, D., Kinne, S., Kondo, Y., Quinn, P. K., Sarofim, M. C., Schultz, M. G.,
1157 Schulz, M., Venkataraman, C., Zhang, H., Zhang, S., Bellouin, N., Guttikunda, S. K., Hopke, P. K.,
1158 Jacobson, M. Z., Kaiser, J. W., Klimont, Z., Lohmann, U., Schwarz, J., PShindell, D., Storelvmo, T.,
1159 Warren, S. G., and Zender, C. S.: Bounding the role of black carbon in the climate system: A
1160 scientific assessment, *J. Geophys Res: Atmos*, 11, 5380-5552, 2013.

1161 Bruce, R. M., Santodonato, J. and Neal, M. W.: Summary Review of the Health Effects Associated
1162 With Phenol, *Toxicol Ind. Health*, 4, 535-568, 1987.

1163 Buha, J., Mueller, N., Nowack, B., Ulrich, A., Losert, S. and Wang, J.: Physical and Chemical
1164 Characterization of Fly Ashes from Swiss Waste Incineration Plants and Determination of the Ash
1165 Fraction in the Nanometer Range, *Environ. Sci. Technol.*, 9, 4765-4773, 2014.

1166 Burkart, K., Nehls, I., Win, T. and Endlicher, W.: The carcinogenic risk and variability of
1167 particulate-bound polycyclic aromatic hydrocarbons with consideration of meteorological conditions,
1168 *Air Quality, Atmos. Health*, 1, 27-38, 2013.

1169 Bzdek, B. R., Ridge, D. P. and Johnston, M. V.: Amine reactivity with charged sulfuric acid clusters,
1170 *Atmos. Chem. Phys.*, 16, 8735-8743, 2011.

1171 Bzdek, B. R., Ridge, D. P. and Johnston, M. V., Amine exchange into ammonium bisulfate and
1172 ammonium nitrate nuclei, *Atmos Chem Phys*, 8:3495-3503, 2010.

1173 Cao, G., Zhang, X. and Zheng, F.: Inventory of black carbon and organic carbon emissions from China,
1174 *Atmos. Environ.*, 34, 6516-6527, 2006.

1175 Cao, G., Zhang, X., Gong, S., An, X. and Wang, Y.: Emission inventories of primary particles and
1176 pollutant gases for China, *Chinese Sci. Bull*, 8, 781-788, 2011.

1177 Cao, G., Zhang, X., Wang, D. and Zheng, F.: Inventory of Emissions of Pollutants from Open Burning
1178 Crop Residues, *J. Agro-Environ. Sci.*, 4, 800-804, 2005.

1179 Cao, J., Xu, H., Xu, Q., Chen, B. and Kan, H.: Fine particulate matter constituents and
1180 cardiopulmonary mortality in a heavily polluted Chinese city, *Environ. Health Persp.*, 3, 373, 2012.

1181 Carlton, A. G., Turpin, B. J., Lim, H., Altieri, K. E. and Seitzinger, S.: Link between isoprene and
1182 secondary organic aerosol (SOA): Pyruvic acid oxidation yields low volatility organic acids in clouds,
1183 *Geophys. Res. Lett.*, L06822, doi:10.1029/2005GL025374, 2006.

1184 Cermak, J. and Knutti, R.: Beijing Olympics as an aerosol field experiment, *Geophys. Res. Lett.*, 36,
1185 L10806, doi:10.1029/2009GL038572, 2009.

1186 Chakrabarty, R. K., Moosmüller, H., Chen, L. W. A., Lewis, K., Arnott, W. P., Mazzoleni, C., Dubey,
1187 M. K., Wold, C. E., Hao, W. M., and Kreidenweis, S. M.: Brown carbon in tar balls from smoldering
1188 biomass combustion, *Atmos. Chem. Phys.*, 13, 6363-6370, 2010.

1189 Chan, M. N., Choi, M. Y., Ng, N. L. and Chan, C. K.: Hygroscopicity of Water-Soluble Organic

1190 Compounds in Atmospheric Aerosols: Amino Acids and Biomass Burning Derived Organic Species,
1191 Environ. Sci. Technol., 6, 1555-1562, 2005.

1192 Chen, H., Hu, D., Wang, L., Mellouki, A. and Chen, J.: Modification in light absorption cross section
1193 of laboratory-generated black carbon-brown carbon particles upon surface reaction and hydration,
1194 Atmos. Environ., 116, 253-261, 2015.

1195 Chen, R., Li, Y., Ma, Y., Pan, G., Zeng, G., Xu, X., Chen, B. and Kan, H.: Coarse particles and
1196 mortality in three Chinese cities: The China Air Pollution and Health Effects Study (CAPES), Sci.
1197 Total Environ., 23, 4934-4938, 2011.

1198 Cheng, Y., Ho, K. F., Lee, S. C. and Law, S. W.: Seasonal and diurnal variations of PM_{1.0}, PM_{2.5} and
1199 PM₁₀ in the roadside environment of Hong Kong, China Particuology, 06:312-315, 2006.

1200 China Ministry of Health (CMH): China statistical yearbook of public health, Peking Union Medical
1201 College Press, 172-189, 2009. (*In Chinese*)

1202 Christopher, S. A., Chou, J., Zhang, J., Li, X., Berendes, T. and Welch, R. M.: Shortwave direct
1203 radiative forcing of biomass burning aerosols estimated using VIRS and CERES data, Geophys. Res.
1204 Lett., 15, 2197-2200, 2000.

1205 Clarke, A., McNaughton, C., Kapustin, V., Shinozuka, Y., Howell, S., Dibb, J., Zhou, J., Anderson, B.,
1206 Brekhovskikh, V., Turner, H. and Pinkerton, M.: Biomass burning and pollution aerosol over North
1207 America: Organic components and their influence on spectral optical properties and humidification
1208 response, J. Geophys. Res., D12, doi:10.1029/2006JD007777, 2007.

1209 Cwiertny, D. M., Baltusaitis, J., Hunter, G. J., Laskin, A., Scherer, M. M. and Grassian, V. H.:
1210 Characterization and acid-mobilization study of iron-containing mineral dust source materials, J.
1211 Geophys. Res.: Atmos., D5, doi:10.1029/2007JD009332, 2008.

1212 Daize, H.: The Utilizing Status and Prospects of the Crop Straw Resources in China, Resource
1213 Development & Market:12, 2000.

1214 Davidson, C. I., Phalen, R. F. and Solomon, P. A.: Airborne Particulate Matter and Human Health: A
1215 Review, Aerosol Sci. Tech., 8, 737-749, 2005.

1216 Delfino, R. J., Sioutas, C. and Malik, S.: Potential role of ultrafine particles in associations between
1217 airborne particle mass and cardiovascular health, Environ. Health Perspect., 8, 934-946, 2005.

1218 Dentener, F. J., Carmichael, G. R., Zhang, Y., Lelieveld, J. and Crutzen, P. J.: Role of mineral aerosol
1219 as a reactive surface in the global troposphere, J. Geophys. Res., D17, 22869-22889, doi:
1220 10.1029/96JD01818, 1996.

1221 Dhammapala, R., Claiborn, C., Corkill, J. and Gullett, B.: Particulate emissions from wheat and
1222 Kentucky bluegrass stubble burning in eastern Washington and northern Idaho, Atmos. Environ., 6,
1223 1007-1015, 2006.

1224 Dhammapala, R., Claiborn, C., Jimenez, J., Corkill, J., Gullett, B., Simpson, C. and Paulsen, M.:
1225 Emission factors of PAHs, methoxyphenols, levoglucosan, elemental carbon and organic carbon from
1226 simulated wheat and Kentucky bluegrass stubble burns, Atmos. Environ., 12, 2660-2669, 2007a.

1227 Dhammapala, R., Claiborn, C., Simpson, C. and Jimenez, J.: Emission factors from wheat and
1228 Kentucky bluegrass stubble burning: Comparison of field and simulated burn experiments, Atmos.
1229 Environ., 7, 1512-1520, 2007b.

1230 Dusek, U., Frank, G. P., Hildebrandt, L., Curtius, J., Schneider, J., Walter, S., Chand, D., Drewnick, F.,
1231 Hings, S., Jung, D.: Size matters more than chemistry for cloud-nucleating ability of aerosol particles,
1232 Science, 5778, 1375-1378, 2006.

1233 Echalar, F., Gaudichet, A., Cachier, H. and Artaxo, P.: Aerosol emissions by tropical forest and

1234 savanna biomass burning: Characteristic trace elements and fluxes, *Geophys. Res. Lett.*, 22, 3039-3042,
1235 doi:10.1029/95GL03170, 1995.

1236 Engelhart, G. J., Hennigan, C. J., Miracolo, M. A., Robinson, A. L. and Pandis, S. N.: Cloud
1237 condensation nuclei activity of fresh primary and aged biomass burning aerosol, *Atmos. Chem. Phys.*,
1238 15, 7285-7293, doi:10.5194/acp-12-7285-2012, 2012.

1239 Falkovich, A. H., E., R. G., G., S., Y., R., Maenhaut, W. and Artaxo, P.: Low molecular weight organic
1240 acids in aerosol particles from Rondônia, Brazil, during the biomass-burning, transition and wet
1241 periods, *Atmos. Chem. Phys.*, 5, 781-797, doi:10.5194/acp-5-781-2005, 2005.

1242 Frey, H. C. and Zhao, Y.: Quantification of Variability and Uncertainty for Air Toxic Emission
1243 Inventories with Censored Emission Factor Data, *Environ. Sci. Technol.*, 22, 6094-6100, 2004.

1244 Frey, H. and Zheng, J.: Quantification of variability and uncertainty in air pollutant emission
1245 inventories: method and case study for utility NO_x emissions, *J. Air Waste Manag. Assoc.*, 9,
1246 1083-1095, 2002.

1247 Fu, H., Zhang, M., Li, W., Chen, J., Wang, L., Quan, X. and Wang, W.: Morphology, composition and
1248 mixing state of individual carbonaceous aerosol in urban Shanghai, *Atmos. Chem. Phys.*, 2, 693-707,
1249 2012.

1250 Galarneau, E.: Source specificity and atmospheric processing of airborne PAHs: Implications for
1251 source apportionment, *Atmos. Environ.*, 35, 8139-8149, 2008.

1252 Gao, M., Guttikunda, S. K., Carmichael, G. R., Wang, Y., Liu, Z., Stanier, C. O., Saide, P. E. and Yu,
1253 M.: Health impacts and economic losses assessment of the 2013 severe haze event in Beijing area, *Sci.*
1254 *Total Environ.*, 511, 553-561, 2015.

1255 Gao, S., Hegg, D. A., Hobbs, P. V., Kirchstetter, T. W., Magi, B. I. and Sadilek, M.: Water-soluble
1256 organic components in aerosols associated with savanna fires in southern Africa: Identification,
1257 evolution, and distribution, *J. Geophys. Res.: Atmos.*, D13, doi:10.1029/2002JD002324, 2003.

1258 Ge, X., Wexler, A. S. and Clegg, S. L.: Atmospheric amines-Part I. A review, *Atmos. Environ.*, 3,
1259 524-546, 2011.

1260 Ghorai, S., Wang, B., Tivanski, A. and Laskin, A.: Hygroscopic Properties of Internally Mixed
1261 Particles Composed of NaCl and Water-Soluble Organic Acids, *Environ. Sci. Technol.*, doi:
1262 10.1021/es404727u, 2014.

1263 Giordano, M., Espinoza, C. and Asa-Awuku, A.: Experimentally measured morphology of biomass
1264 burning aerosol and its impacts on CCN ability, *Atmos. Chem. Phys.*, 4, 1807-1821, 2015.

1265 Grieshop, A. P., Logue, J. M., Donahue, N. M. and Robinson, A. L.: Laboratory investigation of
1266 photochemical oxidation of organic aerosol from wood fires 1: measurement and simulation of organic
1267 aerosol evolution, *Atmos. Chem. Phys.*, 4, 1263-1277, 2009.

1268 Guttikunda, S. K. and Kopakka, R. V.: Source emissions and health impacts of urban air pollution in
1269 Hyderabad, India, *Air Quality, Atmos. & Health*, 2, 195-207, 2014.

1270 Han, Y. M., Chen, L., Huang, R., Chow, J. C., Watson, J. G., Ni, H. Y., Liu, S. X., Fung, K. K., Shen,
1271 Z. X. and Wei, C.: Carbonaceous aerosols in megacity Xi'an, China: Implications of thermal/optical
1272 protocols comparison, *Atmos. Environ.*, 132, 58-68, 2016.

1273 Han, Y. M., Lee, S. C., Cao, J. J., Ho, K. F. and An, Z. S.: Spatial distribution and seasonal variation of
1274 char-EC and soot-EC in the atmosphere over China, *Atmos. Environ.*, 38, 6066-6073, 2009.

1275 Han, Y., Cao, J., Chow, J. C., Watson, J. G., An, Z., Jin, Z., Fung, K. and Liu, S.: Evaluation of the
1276 thermal/optical reflectance method for discrimination between char- and soot-EC, *Chemosphere*, 4,
1277 569-574, 2007.

1278 Hayashi, K., Ono, K., Kajiura, M., Sudo, S., Yonemura, S., Fushimi, A., Saitoh, K., Fujitani, Y. and
1279 Tanabe, K.: Trace gas and particle emissions from open burning of three cereal crop residues: Increase
1280 in residue moistness enhances emissions of carbon monoxide, methane, and particulate organic carbon,
1281 *Atmos. Environ.*, 95, 36-44, 2014.

1282 Hays, M. D., Fine, P. M., Geron, C. D., Kleeman, M. J. and Gullett, B. K.: Open burning of agricultural
1283 biomass: physical and chemical properties of particle-phase emissions, *Atmos. Environ.*, 36,
1284 6747-6764, 2005.

1285 He, K., Zhao, Q., Ma, Y., Duan, F. and Yang, F.: Spatial and seasonal variability of PM_{2.5} acidity at
1286 two Chinese megacities: insights into the formation of secondary inorganic aerosols, *Atmos. Chem.*
1287 *Phys. Dis.*, 25557-25603, doi:10.5194/acpd- 11- 25557- 2011, 2011a.

1288 He, M., Zheng, J., Yin, S. and Zhang, Y.: Trends, temporal and spatial characteristics, and uncertainties
1289 in biomass burning emissions in the Pearl River Delta, China, *Atmos. Environ.*, 24, 4051-4059, 2011b.

1290 Ho, K. F., Ho, S. S. H., Huang, R., Liu, S. X., Cao, J., Zhang, T., Chuang, H., Chan, C. S., Hu, D. and
1291 Tian, L.: Characteristics of water-soluble organic nitrogen in fine particulate matter in the continental
1292 area of China, *Atmos. Environ.*, 106, 252-261, 2015.

1293 Hou, Q., An, X., Wang, Y., Tao, Y. and Sun, Z.: An assessment of China's PM₁₀-related health
1294 economic losses in 2009, *Sci. Total. Environ.*, 61-65, 2012.

1295 Hu, Y., Lin, J., Zhang, S., Kong, L., Fu, H. and Chen, J.: Identification of the typical metal particles
1296 among haze, fog, and clear episodes in the Beijing atmosphere, *Sci. Total Environ.*, 369-380, 2015.

1297 Huang, K., Zhuang, G., Lin, Y., Fu, J. S., Wang, Q., Liu, T., Zhang, R., Jiang, Y., Deng, C. and Fu, Q.:
1298 Typical types and formation mechanisms of haze in an Eastern Asia megacity, Shanghai, *Atmos. Chem.*
1299 *Phys.*, 2012a.

1300 Huang, K., Zhuang, G., Lin, Y., Wang, Q., Fu, J. S., Fu, Q., Liu, T. and Deng, C.: How to improve the
1301 air quality over megacities in China: pollution characterization and source analysis in Shanghai before,
1302 during, and after the 2010 World Expo, *Atmos. Chem. Phys.*, 12, 5927-5942, 2013.

1303 Huang, R., Zhang, Y., Bozzetti, C., Ho, K., Cao, J., Han, Y., Daellenbach, K. R., Slowik, J. G., Platt, S.
1304 M., Canonaco, F., Zotter, P., Wolf, R., Pieber, S., Bruns, E., Crippa, M., Ciarelli, G., Piazzalunga, A.,
1305 Schnelle-Kreis, J., Zimmermann, R., An, Z., Szidat, S., Baltensperger, U., Haddad, I. and Prevot, A.:
1306 High secondary aerosol contribution to particulate pollution during haze events in China, *Nature*, 2014.

1307 Huang, S., Hsu, M. and Chan, C.: Effects of submicrometer particle compositions on cytokine
1308 production and lipid peroxidation of human bronchial epithelial cells., *Environ. Health Persp.*, 4, 478,
1309 2003.

1310 Huang, X., Li, M., Li, J. and Song, Y.: A high-resolution emission inventory of crop burning in fields
1311 in China based on MODIS Thermal Anomalies/Fire products, *Atmos. Environ.*, 9-15, 2012b.

1312 Huo, J., Lu, X., Wang, X., Chen, H., Ye, X., Gao, S., Gross, D. S., Chen, J. and Yang, X.: Online
1313 single particle analysis of chemical composition and mixing state of crop straw burning particles: from
1314 laboratory study to field measurement, *Front Env. Sci. Eng.*, 2, 244-252, 2016.

1315 IBRD and SEPA, Cost of pollution in China: economic estimates of physical damages, 2007, pp.
1316 1-128.

1317 IPCC, Greenhouse Gas Inventory Reference Manual: Revised 2006 IPCC Guidelines for National
1318 Greenhouse Gas Inventories. IPCC/OECD/IES, UK. Meteorological Office, Bracknell, UK., 2007.

1319 IPCC, Quantifying Uncertainties in Practice, Chapter 6: Good Practice Guidance and Uncertainty
1320 Management in National Greenhouse Gas Inventories: In: IES, IPCC, OECD, et al. Bracknell, UK,
1321 1997.

1322 Janssen, N. A. H., Hoek, G., Simic-Lawson, M., Fischer, P., van Bree, L., Ten Brink, H., Keuken, M.,
1323 Atkinson, R., Anderson, H., Brunekreef, B. and Cassee, F.: Black Carbon as an Additional Indicator of
1324 the Adverse Health Effects of Airborne Particles Compared with PM₁₀ and PM_{2.5}, *Environ. Health*
1325 *Persp.*, 12, 1691-1699, 2011.

1326 Jayarathne, T., Stockwell, C. E., Yockelson, R. J., Nakao, S. and Stone, E. A.: Emissions of fine particle
1327 fluoride from biomass burning, *Environ. Sci. Technol.*, 21, 12636-12644, 2014.

1328 Jenkins, B. M., Jones, A. D., Turn, S. Q. and Williams, R. B.: Emission factors for polycyclic aromatic
1329 hydrocarbons from biomass burning, *Environ. Sci. Technol.*, 8, 2462-2469, 1996.

1330 Jickells, T. D., An, Z. S., Andersen, K. K., Baker, A. R., Bergametti, G., J, N. B. J., Duce, R. A.,
1331 Hunter, H., Mahowald, N. and Prospero, A.: Global Iron Connections Between Desert Dust, Ocean
1332 Biogeochemistry, and Climate, *Science*, 308, 67-71, 2005.

1333 Kennedy, I. M.: The health effects of combustion-generated aerosols, *P. Combust Inst*, 2, 2757-2770,
1334 2007.

1335 Kim, K., Jahan, S. A., Kabir, E. and Brown, R. J.: A review of airborne polycyclic aromatic
1336 hydrocarbons (PAHs) and their human health effects, *Environ Int.*, 71-80, 2013.

1337 Kong, L., Yang, Y., Zhang, S., Zhao, X., Du, H., Fu, H., Zhang, S., Cheng, T., Yang, X. and Chen, J.:
1338 Observations of linear dependence between sulfate and nitrate in atmospheric particles, *J. Geophys.*
1339 *Res.: Atmos.*, 1, 341-361, doi:10.1002/2013JD020222, 2014.

1340 Koopmans, A. and Koppejan, J.: Agricultural and forest residue-generation, utilization and availability,
1341 *Modern Applications of Biomass Energy*, 1997.

1342 Korenaga, T., Liu, X. and Huang, Z.: The influence of moisture content on polycyclic aromatic
1343 hydrocarbons emission during rice straw burning, *Chemosphere-Global Change Science*, 1, 117-122,
1344 2001

1345 Kundu, S., Kawamura, K., Andreae, T. W., Hoffer, A. and Andreae, M. O.: Molecular distributions of
1346 dicarboxylic acids, ketocarboxylic acids and α -dicarbonyls in biomass burning aerosols: implications
1347 for photochemical production and degradation in smoke layers, *Atmos. Chem. Phys.*, 5, 2209-2225,
1348 2010.

1349 Laskin, A., Laskin, J. and Nizkorodov, S. A.: Chemistry of atmospheric brown carbon, *Chem. Rev.*, 10,
1350 4335-4382, 2015.

1351 Lavanchy, V. M. H., G Ggeler, H. W., Nyeki, S. and Baltensperger, U.: Elemental carbon (EC) and
1352 black carbon (BC) measurements with a thermal method and an aethalometer at the high-alpine
1353 research station Jungfraujoch, *Atmos. Environ.*, 17, 2759-2769, 1999.

1354 Lee, A. K. Y., Willis, M. D., Healy, R. M., Wang, J. M., Jeong, C. H., Wenger, J. C., Evans, G. J. and
1355 Abbatt, J.: Single particle characterization of biomass burning organic aerosol (BBOA): evidence for
1356 non-uniform mixing of high molecular weight organics and potassium, *Atmos. Chem. Phys. Dis.*, 22,
1357 32157-32183, 2015.

1358 Lee, D. and Wexler, A. S.: Atmospheric amines-Part III: Photochemistry and toxicity, *Atmos. Environ.*,
1359 95-103, 2013.

1360 Lee, R. G. M., Coleman, P., Jones, J. L., Jones, K. C. and Lohmann, R.: Emission Factors and
1361 Importance of PCDD/Fs, PCBs, PCNs, PAHs and PM₁₀ from the Domestic Burning of Coal and Wood
1362 in the U.K., *Environ. Sci. Technol.*, 6, 1436-1447, 2005.

1363 Leng, C., Zhang, Q., Zhang, D., Xu, C., Cheng, T., Zhang, R., Tao, J., Chen, J., Zha, S. and Zhang, Y.:
1364 Variations of cloud condensation nuclei (CCN) and aerosol activity during fog-haze episode: a case
1365 study from Shanghai, *Atmos. Chem. Phys.*, 22, 12499-12512, doi:10.5194/acp-14-12499-2014, 2014.

1366 Lewis, K. A., Arnott, W. P., Moosmuller, H., Chakrabarty, R. K., Carrico, C. M., Kreidenweis, S. M.,
1367 Day, D. E., Malm, W., Laskin, A., Jimenez, J., Ulbrich, I., Huffman, J., Onasch, T., Trimborn, A., Liu,
1368 L. and Mishchenko, M.: Reduction in biomass burning aerosol light absorption upon humidification:
1369 roles of inorganically-induced hygroscopicity, particle collapse, and photoacoustic heat and mass
1370 transfer, *Atmos. Chem. Phys.*, 9, 8949-8966, 2009.

1371 Levin, E. J. T., McMeeking, G. R., Carrico, C. M., Mack, L. E., Kreidenweis, S. M., Wold, C. E.,
1372 Moosmüller, H., Arnott, W., Hao, W., Collett, J. and Malm, W.: Biomass burning smoke aerosol
1373 properties measured during Fire Laboratory at Missoula Experiments (FLAME), *J. Geophys Res.*,
1374 D18210, doi:10.1029/2009JD013601, 2010.

1375 Li, C., Ma, Z., Chen, J., Wang, X., Ye, X., Wang, L., Yang, X., Kan, H., Donaldson, D. and Mellouki,
1376 A.: Evolution of biomass burning smoke particles in the dark, *Atmos. Environ.*, 120, 244-252, 2015.

1377 Li, C., Hu, Y., Chen, J., Ma, Z., Ye, X., Yang, X., Wang, L., Wang, X. and Mellouki, A.:
1378 Physicochemical properties of carbonaceous aerosol from agricultural residue burning: Density,
1379 volatility, and hygroscopicity, *Atmos. Environ.*, 2016.

1380 Li, J., Pósfai, M., Hobbs, P. V. and Buseck, P. R.: Individual aerosol particles from biomass burning in
1381 southern Africa: 2, Compositions and aging of inorganic particles, *J. Geophys. Res.: Atmos.*,
1382 (1984-2012), D13, doi:10.1029/2002JD002310, 2003.

1383 Li, X., Wang, S., Duan, L., Hao, J., Li, C., Chen, Y. and Yang, L.: Particulate and trace gas emissions
1384 from open burning of wheat straw and corn stover in China, *Environ. Sci. Technol.*, 17, 6052-6058,
1385 2007.

1386 Lima, A. L. C., Farrington, J. W. and Reddy, C. M.: Combustion-Derived Polycyclic Aromatic
1387 Hydrocarbons in the Environment-A Review, *Environ. Forensics.*, 2, 109-131, 2005.

1388 Lin, J., Nielsen, C. P., Zhao, Y., Lei, Y., Liu, Y. and McElroy, M. B.: Recent changes in particulate air
1389 pollution over China observed from space and the ground: effectiveness of emission control, *Environ.*
1390 *Sci. Technol.*, 20, 7771-7776, 2010.

1391 Lin, P., Aiona, P. K., Li, Y., Shiraiwa, M., Laskin, J., Nizkorodov, S. A. and Laskin, A.: Molecular
1392 Characterization of Brown Carbon in Biomass Burning Aerosol Particles, *Environ. Sci. Technol.*, 21,
1393 11815-11824, 2016.

1394 Liu, M., Song, Y., Yao, H., Kang, Y., Li, M., Huang, X. and Hu, M.: Estimating emissions from
1395 agricultural fires in the North China Plain based on MODIS fire radiative power, *Atmos. Environ.*,
1396 326-334, 2015.

1397 Liu, Q. and Bei, Y.: Impacts of crystal metal on secondary aliphatic amine aerosol formation during
1398 dust storm episodes in Beijing, *Atmos. Environ.*, 227-234, 2016.

1399 Lobert, J. M., Scharffe, D. H., Hao, W. M. and Crutzen, P. J.: Importance of biomass burning in the
1400 atmospheric budgets of nitrogen-containing gases, *6284*, 552-554, 1990.

1401 Lu, Z., Zhang, Q. and Streets, D. G.: Sulfur dioxide and primary carbonaceous aerosol emissions in
1402 China and India, 1996-2010, *Atmos. Chem. Phys.*, 11, 9839-9864, doi:10.5194/acp-11-9839-2011,
1403 2011.

1404 Ma, J. and Van Aardenne, J. A.: Impact of different emission inventories on simulated tropospheric
1405 ozone over China: a regional chemical transport model evaluation, *Atmos. Chem. Phys.*, 4, 877-887,
1406 2004.

1407 May, A. A., McMeeking, G. R., Lee, T., Taylor, J. W., Craven, J. S., Burling, I., Sullivan, A. P., Akagi,
1408 S., Collett, J., Flynn, M., Coe, H., Urbanski, S., Seinfeld, J., Yokelson, R. and Kreidenweis, S.: Aerosol
1409 emissions from prescribed fires in the United States: A synthesis of laboratory and aircraft

1410 measurements, *J. Geophys. Res.: Atmos.*, 20, 11826-11849, doi:10.1002/2014JD021848, 2014.

1411 Meskhidze, N.: Dust and pollution: A recipe for enhanced ocean fertilization? *J. Geophys. Res.*, D3,
1412 doi:10.1029/2004JD005082, 2005.

1413 Mikhailov, E. F., Vlasenko, S. S., Podgorny, I. A., Ramanathan, V. and Corrigan, C. E.: Optical
1414 properties of soot-water drop agglomerates: An experimental study, *J. Geophys. Res.*, 111, D07209,
1415 doi:10.1029/2005JD006389, 2006.

1416 Moreno, T., Karanasiou, A., Amato, F., Lucarelli, F., Nava, S., Calzolari, G., Chiari, M., Coz, E.,
1417 Artinano, B., Lumberras, J., Borge, R., Boldo, R., Linares, C., Alastursy, A., Querol, X. and Gibbons,
1418 X.: Daily and hourly sourcing of metallic and mineral dust in urban air contaminated by traffic and
1419 coal-burning emissions, *Atmos. Environ.*, 68, 33-44, 2013.

1420 NBSC, China Statistical Yearbook 2013: China Statistics Press Beijing, China, 2013.

1421 NHFPC, National Health and Family Planning Yearbook: Peking Union Medical College Press, 2013,
1422 p. 415.

1423 Oanh, N. T. K., Ly, B. T., Tipayarom, D., Manandhar, B. R., Prapat, P., Simpson, C. D. and Liu, L. S.:
1424 Characterization of particulate matter emission from open burning of rice straw, *Atmos. Environ.*, 2,
1425 493-502, 2011.

1426 Ostro, B. and Chestnut, L.: Assessing the health benefits of reducing particulate matter air pollution in
1427 the United States, *Environ. Res.*, 2, 94-106, 1998.

1428 Pope III, C. A., Burnett, R. T., Thun, M. J., Calle, E. E., Krewski, D., Ito, K. and Thurston, G. D.: Lung
1429 cancer, cardiopulmonary mortality, and long-term exposure to fine particulate air pollution, *Jama*, 9,
1430 1132-1141, 2002.

1431 Pope, C. A., Burnett, R. T., Thurston, G. D., Thun, M. J., Calle, E. E., Krewski, D. and Godleski, J. J.:
1432 Cardiovascular mortality and long-term exposure to particulate air pollution epidemiological evidence
1433 of general pathophysiological pathways of disease, *Circulation*, 1, 71-77, 2004.

1434 Pósfai, M.: Atmospheric tar balls: Particles from biomass and biofuel burning, *J. Geophys. Res.*, 109,
1435 D06213, doi:10.1029/2003JD004169, 2004.

1436 Qin, Y. and Xie, S. D.: Spatial and temporal variation of anthropogenic black carbon emissions in
1437 China for the period 1980-2009, *Atmos. Chem. Phys.*, 11, 4825-4841, 2012.

1438 Qin, Y. and Xie, S. D.: Historical estimation of carbonaceous aerosol emissions from biomass open
1439 burning in China for the period 1990-2005, *Environ. Pollut.*, 12, 3316-3323, 2011.

1440 Qiu, C. and Zhang, R.: Physicochemical Properties of Alkylammonium Sulfates: Hygroscopicity,
1441 Thermostability, and Density, *Environ. Sci. Technol.*, 8, 4474-4480, 2012.

1442 Qiu, C., Wang, L., Lal, V., Khalizov, A. F. and Zhang, R.: Heterogeneous Reactions of Alkylamines
1443 with Ammonium Sulfate and Ammonium Bisulfate, *Environ. Sci. Technol.*, 11, 4748-4755, 2011.

1444 Ram, K., Sarin, M. M. and Tripathi, S. N.: Temporal Trends in Atmospheric PM_{2.5}, PM₁₀, Elemental
1445 Carbon, Organic Carbon, Water-Soluble Organic Carbon, and Optical Properties: Impact of Biomass
1446 Burning Emissions in The Indo-Gangetic Plain, *Environ. Sci. Technol.*, 2, 686-695, 2011.

1447 Ram, K. and Sarin, M. M.: Day-night variability of EC, OC, WSOC and inorganic ions in urban
1448 environment of Indo-Gangetic Plain: implications to secondary aerosol formation, *Atmos. Environ.*, 2,
1449 460-468, 2011.

1450 Reddy, M. S. and Venkataraman, C.: Atmospheric optical and radiative effects of anthropogenic
1451 aerosol constituents from India, *Atmos. Environ.*, 34, 4511-4523, 2000.

1452 Reid, J. S., Eck, T. F., Christopher, S. A., Koppmann, R., Dubovik, O., Eleuterio, D. P., Holben, B. N.,
1453 Reid, E. A. and Zhang, J.: A review of biomass burning emissions part III: intensive optical properties

1454 of biomass burning particles, *Atmos. Chem. Phys.*, 5, 827-849, 2005a.

1455 Reid, J. S., Koppmann, R., Eck, T. F. and Eleuterio, D. P.: A review of biomass burning emissions part
1456 II: intensive physical properties of biomass burning particles, *Atmos. Chem. Phys.*, 3, 799-825, 2005b.

1457 Richter, H. and J, H.: Formation of polycyclic aromatic hydrocarbons and their growth to soot-a review
1458 of chemical reaction pathways, *Prog Energ Combust*, 4, 565-608, 2000.

1459 Ripoll, A., Minguillón, M. C., Pey, J., Pérez, N., Querol, X. and Alastuey, A.: Joint analysis of
1460 continental and regional background environments in the western Mediterranean: PM₁ and PM₁₀
1461 concentrations and composition, *Atmos. Chem. Phys.*, 2, 1129-1145, doi:10.5194/acp-15-1129-2015,
1462 2015.

1463 Roemer, W. H. and van Wijnen, J. H.: Differences among Black Smoke, PM₁₀, and PM_{1.0} Levels at
1464 Urban Measurement Sites, *Environ. Health Persp.*, 2, 151-153, 2001.

1465 Rose, D., Gunthe, S. S., Su, H., Garland, R. M., Yang, H., Berghof, M., Cheng, Y. F., Wehner, B.,
1466 Achtert, P., Nowak, A., Wiedensohler, A., Takegawa, N., Kondo, Y., Hu, M., Zhang, Y., Andreae, M.
1467 and Poschl, U.: Cloud condensation nuclei in polluted air and biomass burning smoke near the
1468 mega-city Guangzhou, China-Part 2: Size-resolved aerosol chemical composition, diurnal cycles, and
1469 externally mixed weakly CCN-active soot particles, *Atmos. Chem. Phys.*, 6, 2817-2836,
1470 doi:10.5194/acp-11-2817-2011, 2011.

1471 Rosenfeld, D.: Atmosphere: Aerosols, Clouds, and Climate, *Science*, 5778, 1323-1324, 2006.

1472 Safai, P. D., Raju, M. P., Budhavant, K. B., Rao, P. and Devara, P.: Long term studies on
1473 characteristics of black carbon aerosols over a tropical urban station Pune, India, *Atmos. Res.*, 173-184,
1474 2013.

1475 Saffari, A., Daher, N., Samara, C., Voutsas, D., Kouras, A., Manoli, E., Karagkiozidou, O.,
1476 Vlachokostas, C., Moussiopoulos, N., Shafer, M., Schauer, J. and Sioutas, C.: Increased Biomass
1477 Burning Due to the Economic Crisis in Greece and Its Adverse Impact on Wintertime Air Quality in
1478 Thessaloniki, *Environ. Sci. Technol.*, 23, 13313-13320, 2013.

1479 Saikawa, E., Naik, V., Horowitz, L. W., Liu, J. and Mauzerall, D. L.: Present and potential future
1480 contributions of sulfate, black and organic carbon aerosols from China to global air quality, premature
1481 mortality and radiative forcing, *Atmos. Environ.*, 17, 2814-2822, 2009.

1482 Samy, S. and Hays, M. D.: Quantitative LC-MS for water-soluble heterocyclic amines in fine aerosols
1483 (PM_{2.5}) at Duke Forest, USA, *Atmos. Environ.*, 77-80, 2013.

1484 Santodonato, J.: Review of the estrogenic and antiestrogenic activity of polycyclic aromatic
1485 hydrocarbons: relationship to carcinogenicity, *Chemosphere*, 4, 835-848, 1997.

1486 Schade, G. W. and Crutzen, P. J.: Emission of aliphatic amines from animal husbandry and their
1487 reactions: Potential source of N₂O and HCN, *J. Atmos. Chem.*, 3, 319-346, 1995.

1488 Schauer, J. J., Kleeman, M. J., Cass, G. R. and Simoneit, B. R. T.: Measurement of Emissions from Air
1489 Pollution Sources. 3. C1-C29 Organic Compounds from Fireplace Combustion of Wood, *Environ. Sci.*
1490 *Technol.*, 9, 1716-1728, 2001.

1491 Schlesinger, R. B.: Comparative deposition of inhaled aerosols in experimental animals and humans: a
1492 review, *Journal of Toxicology and Environmental Health, Part A Current Issues*, 2, 197-214, 1985.

1493 Seinfeld, J. H. and Pandis, S. N.: Atmospheric chemistry and physics: from air pollution to climate
1494 change: John Wiley & Sons, 2012.

1495 Sen, A., Mandal, T. K., Sharma, S. K., Saxena, M., Gupta, N. C., Gautam, R., Gupta, A., Gill, T., Rani,
1496 S., Saud, T., Singh, D. and Gadi, R.: Chemical properties of emission from biomass fuels used in the
1497 rural sector of the western region of India, *Atmos. Environ.*, 411-424, 2014.

1498 Shi, Y., Chen, J., Hu, D., Wang, L., Yang, X. and Wang, X.: Airborne submicron particulate (PM₁)
1499 pollution in Shanghai, China: Chemical variability, formation/dissociation of associated semi-volatile
1500 components and the impacts on visibility, *Sci. Total. Environ.*, 199-206, 2014.

1501 Shindell, D., Kuylensstierna, J. C. I., Vignati, E., van Dingenen, R., Amann, M., Klimont, Z., Anenberg,
1502 S. C., Muller, N., Janssens-Maenhout, G., Raes, F., Schwartz, J., Faluvegi, G., Pozzoli, L., Kupiainen,
1503 K., Hoglund-Isaksson, L., Emberson, L., Streets, D., Ramanathan, V., Hicks, K., Oanh, N., Milly, G.,
1504 Williams, M., Demkin, V. and Fowler, D.: Simultaneously Mitigating Near-Term Climate Change and
1505 Improving Human Health and Food Security, *Science*, 6065, 183-189, 2012.

1506 Simcik, M. F., Eisenreich, S. J. and Lioy, P. J.: Source apportionment and source/sink relationships of
1507 PAHs in the coastal atmosphere of Chicago and Lake Michigan, *Atmos. Environ.*, 30, 5071-5079,
1508 1999.

1509 Simoneit, B. R. T., Rushdi, A. I., Bin Abas, M. R. and Didyk, B. M.: Alkyl Amides and Nitriles as
1510 Novel Tracers for Biomass Burning, *Environ. Sci. Technol.*, 1, 16-21, 2003.

1511 Streets, D. G.: Dissecting future aerosol emissions: Warming tendencies and mitigation opportunities,
1512 *Climatic Change*, 3-4, 313-330, 2007.

1513 Sun, J., Peng, H., Chen, J., Wang, X., Wei, M., Li, W., Yang, L., Zhang, L., Wang, W. and Mellouki,
1514 A.: An estimation of CO₂ emission via agricultural crop residue open field burning in China from 1996
1515 to 2013, *J. Clean Prod.*, 2625-2631, 2016.

1516 Takegawa, N., Miyakawa, T., Kawamura, K. and Kondo, Y.: Contribution of Selected Dicarboxylic
1517 and ω-Oxocarboxylic Acids in Ambient Aerosol to the m/z 44 Signal of an Aerodyne Aerosol Mass
1518 Spectrometer, *AerosolSci. Tech.*, 41, 418-437, 2007.

1519 Tao, Y., Ye, X., Jiang, S., Yang, X., Chen, J., Xie, Y. and Wang, R.: Effects of amines on particle
1520 growth observed in new particle formation events, *J. Geophys. Res.: Atmos.*, 121, 324-335,
1521 doi:10.1002/2015JD024245, 2016.

1522 Tian, D., Hu, Y., Wang, Y., Boylan, J. W., Zheng, M. and Russell, A. G.: Assessment of Biomass
1523 Burning Emissions and Their Impacts on Urban and Regional PM_{2.5}: A Georgia Case Study, *Environ*
1524 *Sci. Technol.*, 2, 299-305, 2008.

1525 Tóth, A., Hoffer, A., Nyirő-Kósa, I., Pósfai, M. and Gelencsér, A.: Atmospheric tar balls: aged primary
1526 droplets from biomass burning? *Atmos. Chem. Phys. Dis.*, 12, 33089-33104, doi:10.5194/acp-14-
1527 6669-2014, 2013.

1528 Tsai, P. J., Shieh, H. Y., Lee, W. J. and Lai, S. O.: Health-risk assessment for workers exposed to
1529 polycyclic aromatic hydrocarbons (PAHs) in a carbon black manufacturing industry, *Sci. Total.*
1530 *Environ.*, 1-3, 137-150, 2001.

1531 Urban, R. C., Alves, C. A., Allen, A. G., Cardoso, A. A. and Campos, M.: Organic aerosols in a
1532 Brazilian agro-industrial area: Speciation and impact of biomass burning, *Atmos. Res.*, 271-279, 2016.

1533 Veres, P., Roberts, J. M., Burling, I. R., Warneke, C., de Gouw, J. and Yokelson, R. J.: Measurements
1534 of gas-phase inorganic and organic acids from biomass fires by negative-ion proton-transfer
1535 chemical-ionization mass spectrometry, *J. Geophys Res.*, 115, D23302, doi:10.1029/2010JD014033,
1536 2010.

1537 Wang, L., Li, X. and Xu, Y.: The Economic Losses Caused By Crop Residues Burnt in Open Field in
1538 China, *J. Arid Land Resources and Environment*, 2, 170-175, 2008a.

1539 Wang, R., Tao, S., Wang, W., Liu, J., Shen, H., Shen, G., Wang, B., Liu, X., Li, W., Huang, Y., Zhang,
1540 Y., Lu, Y., Chen, H., Chen, Y., Wang, C., Zhu, D., Wang, X., Li, B., Liu, W., Ma, J. and Prospero, A.:
1541 Black carbon emissions in China from 1949 to 2050, *Environ. Sci. Technol.*, 14, 7595-7603, 2012.

1542 Wang, S. and Zhang, C.: Spatial and temporal distribution of air pollutant emissions from open burning
1543 of crop residues in China, Sciencepaper Online, 5:329-333, 2008b.(*in chinese*)

1544 Wang, S., Zhao, M., Xing, J., Wu, Y., Zhou, Y., Lei, Y., He, K., Fu, L. and Hao, J.: Quantifying the air
1545 pollutants emission reduction during the 2008 Olympic Games in Beijing, Environ. Sci. Technol., 7,
1546 2490-2496, 2010.

1547 Wang, W., Jariyasopit, N., Schrlau, J., Jia, Y., Tao, S., Yu, T., Dashwood, R. H., Zhang, W., Wang, X.
1548 and Simonich, S.: Concentration and photochemistry of PAHs, NPAHs, and OPAHs and toxicity of
1549 PM_{2.5} during the Beijing Olympic Games, Environ. Sci. Technol., 16, 6887-6895, 2011.

1550 Wei, B. and Yang, L.: A review of heavy metal contaminations in urban soils, urban road dusts and
1551 agricultural soils from China, Microchem J., 2, 99-107, 2010.

1552 Wei, W., Jitao, Y., Qingling, Z. and Bailiang, Z.: Current Situation and Developing Direction of Straw
1553 Utilization Technology in China, China Resources Comprehensive Utilization, 11, 2004.

1554 WHO, Life Database in 2000, World Health Organization, 2000.

1555 Wilson, J. M., Baeza-Romero, M. T., Jones, J. M., Pourkashanian, M., Williams, A., Lea-Langton, A.
1556 R., Ross, A. B. and Bartle, K.: Soot Formation from the Combustion of Biomass Pyrolysis Products
1557 and a Hydrocarbon Fuel, n-Decane: An Aerosol Time Of Flight Mass Spectrometer (ATOFMS) Study,
1558 Energ Fuel, 3, 1668-1678, 2013.

1559 Wong, C., Vichit-Vadakan, N., Kan, H., Qian, Z. and Teams, T. P. P.: Public Health and Air Pollution
1560 in Asia (PAPA): A Multicity Study of Short-Term Effects of Air Pollution on Mortality, Environ.
1561 Health Persp., 9, 1195-1202, 2008.

1562 Wu, C., Liu, L. J. S., Cullen, A., Westberg, H. and Williamson, J., Spatial-temporal and cancer risk
1563 assessment of selected hazardous air pollutants in Seattle, Environ Int., 1, 11-17, 2011.

1564 Wu, C., Wu, S., Wu, Y., Cullen, A. C., Larson, T. V., Williamson, J. and Liu, L. J. S.: Cancer risk
1565 assessment of selected hazardous air pollutants in Seattle, Environ Int., 3, 516-522, 2009.

1566 Xu, S., Liu, W. and Tao, S.: Emission of Polycyclic Aromatic Hydrocarbons in China, Environ Sci.
1567 Technol., 3, 702-708, 2006.

1568 Yang, C., Peng, X., Huang, W., Chen, R., Xu, Z., Chen, B. and Kan, H. . A time-stratified
1569 case-crossover study of fine particulate matter air pollution and mortality in Guangzhou, China, Int
1570 Arch. Occ. Env. Hea., 5, 579-585, 2012.

1571 Yang, M., Howell, S. G., Zhuang, J. and Huebert, B. J.: Attribution of aerosol light absorption to black
1572 carbon, brown carbon, and dust in China-interpretations of atmospheric measurements during
1573 EAST-AIRE, Atmos. Chem. Phys., 6, 2035-2050, doi:10.5194/acp-9-2035-2009, 2009.

1574 Yang, Y., Liu, X., Qu, Y., Wang, J., An, J., Zhang, Y. and Zhang, F.: Formation mechanism of
1575 continuous extreme haze episodes in the megacity Beijing, China, in January 2013, Atmos. Res.,
1576 192-203, 2015.

1577 Yokelson, R. J., Karl, T., Artaxo, P. and Blake, D. R.: The Tropical Forest and Fire Emissions
1578 Experiment: overview and airborne fire emission factor measurements, Atmos. Chem. Phys., 7,
1579 5175-5196, doi:10.5194/acp-7-5175-2007, 2007.

1580 Yunker, M. B., Macdonald, R. W., Vingarzan, R., Mitchell, R. H., Goyette, D. and Sylvestre, S.: PAHs
1581 in the Fraser River basin: a critical appraisal of PAH ratios as indicators of PAH source and
1582 composition, Org Geochem, 4, 489-515, 2002.

1583 Zhang, H., Hu, D., Chen, J., Ye, X., Wang, S. X., Hao, J. M., Wang, L., Zhang, R. and An, Z.: Particle
1584 Size Distribution and Polycyclic Aromatic Hydrocarbons Emissions from Agricultural Crop Residue
1585 Burning, Environ. Sci. Technol., 13, 5477-5482, 2011.

1586 Zhang, H., Wang, S., Hao, J., Wan, L., Jiang, J., Zhang, M., Mestl, H. E., Mestl, H., Alnes, L., Aunan,
1587 K. and Mellouki, A.: Chemical and size characterization of particles emitted from the burning of coal
1588 and wood in rural households in Guizhou, China, *Atmos. Environ.*, 94-99, 2012.

1589 Zhang, H., Ye, X., Cheng, T., Chen, J., Yang, X., Wang, L. and Zhang, R.: A laboratory study of
1590 agricultural crop residue combustion in China: Emission factors and emission inventory, *Atmos.*
1591 *Environ.*, 36, 8432-8441, 2008a.

1592 Zhang, R., Khalizov, A. F., Pagels, J., Zhang, D., Xue, H. and McMurry, P. H.: Variability in
1593 morphology, hygroscopicity, and optical properties of soot aerosols during atmospheric processing,
1594 *Proc Natl Acad Sci USA*, 30, 10291-10296, 2008b.

1595 Zhang, R., Suh, I., Zhao, J., Zhang, D., Fortner, E. C., Tie, X., Molina, L. T. and Molina, M. J.:
1596 Atmospheric new particle formation enhanced by organic acids, *Science*, 5676, 1487-1490, 2004.

1597 Zhao, B., Wang, P., Ma, J. Z., Zhu, S., Pozzer, A. and Li, W.: A high-resolution emission inventory of
1598 primary pollutants for the Huabei region, China, *Atmos. Chem. Phys.*, 1, 481-501, 2012.

1599 Zhao, Y., Nielsen, C. P., Lei, Y., McElroy, M. B. and Hao, J.: Quantifying the Uncertainties of a
1600 Bottom-Up Emission Inventory of Anthropogenic Atmospheric Pollutants in China, *Atmos. Chem.*
1601 *Phys.*, 11, 2295-2308, 2011.

1602 Zheng, J., Ma, Y., Chen, M., Zhang, Q., Wang, L., Khalizov, A. F., Yao, L., Wang, Z., Wang, X. and
1603 Chen, L.: Measurement of atmospheric amines and ammonia using the high resolution time-of-flight
1604 chemical ionization mass spectrometry, 249-259, 2015.

1605

1606

1607 **Tables and figure captions**

1608 **Table 1.** Emission factors of particulate chemical species in smoke PM_{2.5} from
1609 agricultural residue burning (mean value ± standard deviation).

1610 **Table 2.** Emission factors of particulate chemical species in smoke PM_{1.0} from
1611 agricultural residue burning (mean value ± standard deviation).

1612 **Table 3.** Comparison of emission factors with literature (specific chemical materials
1613 in form of PM_{2.5})

1614 **Table 4.** Summary of field burning rates and economic data in China

1615 **Table 5.** National agricultural field burning emissions of BAU, EM, and NDRC
1616 scenarios in China, 2012.

1617 **Table 6.** Uncertainties for national smoke aerosol emissions in 2012.

1618 **Table 7.** Estimated number of cases (95% CI) attributable to agricultural fire smoke
1619 PM_{2.5} exposure in China, 2012

1620 **Table 8.** Health-related economic loss (95% CI) from agricultural fire smoke PM_{2.5}
1621 exposure in China, 2012

1622 **Figure 1.** Schematic methodology for developing emission estimations

1623 **Figure 2.** Chemical profiles of smoke PM_{2.5} and PM_{1.0} from 5 types agricultural
1624 residue burnings. OM (organic matter = 1.3×OC). OWSI, other water soluble ions
1625 including F⁻, NO₂⁻, Na⁺, Ca²⁺, Mg²⁺.

1626 **Figure 3.** a) Emission factors of 16 USEPA priority PAHs in smoke PM_{2.5} and PM_{1.0};
1627 b) expulsion-accumulation of PAHs in OC-EC of smoke PM_{2.5} and PM_{1.0}

1628 **Figure 4.** Transmission electron microscope (TEM) images and EDX analysis of
1629 fresh agricultural residue burning particles. (a)-(c) Crystal and amorphous KCl
1630 particles internally mixed with sulfate, nitrate, and carbonaceous materials. (d)-(f)
1631 Heavy metal-bearing fractal-like fly ash particles. (e)-(g) Chain-like soot particles and
1632 tar ball.

1633 **Figure 5.** Annual agricultural residue production of five major crops and allocated
1634 into two harvest (summer and autumn harvest) based on agricultural yield in China,
1635 2012.

1636 **Figure 6.** Statistical analysis of field burning rates from BAU, EM, and NDRC
1637 versions

1638 **Figure 7.** Spatial and temporal distribution of smoke PM_{2.5} emissions and flux
1639 concentrations from agricultural field burning over China, 2012

1640 **Figure 8.** Nationwide $PM_{2.5}$ emissions and flux concentrations based on different
1641 burning versions. The inset pie-graphs are chemical compositions of integrated $PM_{2.5}$
1642 from five major agricultural residue burning.

1643

1644
1645

Table 1. Emission factors of particulate chemical species in smoke PM_{2.5} from agricultural residue burning (mean value ± standard deviation).

Chemical Species (g kg ⁻¹)	wheat straw	corn straw	rice straw	cotton residue	soybean residue
PM _{2.5}	5.803 ± 0.363	5.988 ± 0.723	14.732 ± 2.417	15.162 ± 2.053	3.249 ± 0.350
OC	2.813 ± 0.147	2.393 ± 0.351	6.882 ± 0.689	7.415 ± 0.547	1.539 ± 0.253
EC	0.676 ± 0.027	0.778 ± 0.152	2.182 ± 0.278	1.192 ± 0.171	0.614 ± 0.190
Inorganic ions (g kg⁻¹)	1.273 ± 0.072	1.810 ± 0.030	3.086 ± 0.266	3.810 ± 0.246	0.523 ± 0.149
SO ₄ ²⁻	0.084 ± 0.028	0.217 ± 0.041	0.409 ± 0.127	0.701 ± 0.081	0.073 ± 0.014
Cl ⁻	0.576 ± 0.038	0.709 ± 0.034	1.158 ± 0.232	1.351 ± 0.114	0.178 ± 0.030
F ⁻	0.023 ± 0.061	0.061 ± 0.005	0.073 ± 0.024	0.265 ± 0.012	0.009 ± 0.004
NO ₃ ⁻	0.023 ± 0.000	0.032 ± 0.002	0.051 ± 0.025	0.072 ± 0.004	0.009 ± 0.004
NO ₂ ⁻	0.006 ± 0.001	0.016 ± 0.002	0.018 ± 0.002	0.036 ± 0.001	0.004 ± 0.003
Ca ²⁺	0.030 ± 0.011	0.036 ± 0.003	0.046 ± 0.007	0.060 ± 0.003	0.010 ± 0.002
Na ⁺	0.005 ± 0.001	0.012 ± 0.001	0.028 ± 0.004	0.050 ± 0.004	0.005 ± 0.001
NH ₄ ⁺	0.152 ± 0.005	0.197 ± 0.010	0.542 ± 0.107	0.347 ± 0.008	0.029 ± 0.004
Mg ²⁺	0.005 ± 0.000	0.017 ± 0.002	0.023 ± 0.004	0.032 ± 0.002	0.005 ± 0.001
K ⁺	0.368 ± 0.041	0.514 ± 0.009	0.739 ± 0.049	0.947 ± 0.070	0.200 ± 0.023
Organic Acids (mg kg⁻¹)	156.680 ± 81.830	46.670 ± 9.000	557.130 ± 269.380	769.990 ± 317.550	143.310 ± 39.770
CH ₃ COOH	148.900 ± 79.290	36.640 ± 8.210	417.930 ± 186.140	743.320 ± 159.600	135.500 ± 62.320
MSA	7.170 ± 2.110	10.030 ± 30.000	136.990 ± 81.700	12.980 ± 1.530	3.200 ± 1.530
H ₂ C ₂ O ₄	2.610 ± 0.430	ND	2.210 ± 1.560	4.760 ± 2.640	2.170 ± 2.380
HCOOH	ND	ND	ND	8.930 ± 2.630	2.440 ± 1.450
Amine salts (mg kg⁻¹)	19.246 ± 9.368	32.877 ± 19.141	104.787 ± 15.635	102.409 ± 13.379	4.514 ± 1.776
MeOH ⁺ + MMAH ⁺	1.322 ± 0.086	5.735 ± 0.102	17.226 ± 1.454	19.888 ± 0.351	0.456 ± 0.196
MEAH ⁺	0.201 ± 0.055	0.675 ± 0.135	4.175 ± 0.920	3.690 ± 1.959	ND
TEOH ⁺	2.562 ± 0.962	4.118 ± 0.741	25.129 ± 0.343	14.376 ± 8.688	0.672 ± 0.558
DEAH ⁺ + TMAH ⁺	13.728 ± 7.512	18.973 ± 0.466	46.148 ± 12.185	28.568 ± 5.321	2.012 ± 0.878
DMAH ⁺	1.434 ± 0.925	3.376 ± 0.674	12.110 ± 6.166	35.887 ± 2.940	1.374 ± 0.144
Elemental Species (mg kg⁻¹)	53.813 ± 18.860	53.546 ± 9.070	131.612 ± 5.920	27.577 ± 3.700	14.003 ± 8.710
Phenols (mg kg⁻¹)	26.785 ± 8.582	16.390 ± 2.652	27.238 ± 4.861	41.481 ± 5.517	9.673 ± 2.272
PAHs (mg kg⁻¹)	1.814 ± 0.348	2.706 ± 0.798	7.267 ± 1.722	8.302 ± 2.856	1.832 ± 0.353

1646

ND means not detected

1647
1648

Table 2. Emission factors of particulate chemical species in smoke PM_{1.0} from agricultural residue burning (mean value ± standard deviation).

Chemical Species (g kg ⁻¹)	wheat straw	corn straw	rice straw	cotton residue	soybean residue
PM _{1.0}	5.298 ± 0.295	5.360 ± 0.551	13.200 ± 1.440	12.635 ± 1.243	3.036 ± 0.257
OC	2.419 ± 0.126	2.063 ± 0.340	6.024 ± 0.602	6.036 ± 0.360	1.338 ± 0.128
EC	0.650 ± 0.037	0.728 ± 0.122	2.083 ± 0.413	1.023 ± 0.205	0.575 ± 0.260
Inorganic ions (g kg⁻¹)	1.215 ± 0.040	1.768 ± 0.010	2.940 ± 0.249	3.516 ± 0.145	0.510 ± 0.156
SO ₄ ²⁻	0.078 ± 0.011	0.199 ± 0.032	0.333 ± 0.107	0.581 ± 0.054	0.073 ± 0.056
Cl ⁻	0.544 ± 0.033	0.712 ± 0.027	1.145 ± 0.118	1.243 ± 0.067	0.175 ± 0.031
F ⁻	0.022 ± 0.007	0.041 ± 0.004	0.078 ± 0.030	0.151 ± 0.011	0.001 ± 0.001
NO ₃ ⁻	0.021 ± 0.005	0.027 ± 0.002	0.043 ± 0.016	0.061 ± 0.003	0.009 ± 0.002
NO ₂ ⁻	0.006 ± 0.001	0.010 ± 0.003	0.013 ± 0.004	0.019 ± 0.002	0.004 ± 0.003
Ca ²⁺	0.027 ± 0.013	0.028 ± 0.002	0.045 ± 0.008	0.067 ± 0.005	0.010 ± 0.002
Na ⁺	0.004 ± 0.000	0.012 ± 0.000	0.027 ± 0.003	0.056 ± 0.006	0.005 ± 0.002
NH ₄ ⁺	0.147 ± 0.005	0.191 ± 0.009	0.511 ± 0.067	0.401 ± 0.004	0.031 ± 0.005
Mg ²⁺	0.005 ± 0.001	0.035 ± 0.001	0.024 ± 0.006	0.033 ± 0.002	0.005 ± 0.001
K ⁺	0.359 ± 0.040	0.513 ± 0.015	0.721 ± 0.073	0.994 ± 0.067	0.197 ± 0.035
Organic Acids (mg kg⁻¹)	124.310 ± 25.170	47.830 ± 10.610	427.400 ± 221.270	639.820 ± 244.960	130.760 ± 59.310
CH ₃ COOH	115.790 ± 21.940	38.960 ± 9.610	383.360 ± 179.050	615.790 ± 232.860	124.310 ± 69.000
MSA	6.830 ± 2.030	8.870 ± 2.730	41.380 ± 38.480	11.380 ± 2.360	3.200 ± 1.730
H ₂ C ₂ O ₄	1.690 ± 1.200	ND	2.660 ± 1.760	3.620 ± 1.250	1.560 ± 1.670
HCOOH	ND	ND	ND	9.030 ± 7.710	1.690 ± 1.390
Amine salts (mg kg⁻¹)	18.191 ± 5.351	29.891 ± 13.480	81.726 ± 11.455	85.720 ± 21.337	4.385 ± 1.445
MeOH ⁺ + MMAH ⁺	1.300 ± 0.282	5.647 ± 0.342	16.627 ± 0.104	18.834 ± 1.991	0.464 ± 0.265
MEAH ⁺	0.157 ± 0.037	0.787 ± 0.211	3.581 ± 0.602	2.771 ± 1.304	ND
TEOH ⁺	1.719 ± 0.283	5.115 ± 0.732	17.575 ± 0.844	11.441 ± 3.229	0.529 ± 0.304
DEAH ⁺ + TMAH ⁺	13.716 ± 9.047	15.921 ± 1.620	33.565 ± 6.795	29.057 ± 3.793	2.278 ± 0.533
DMAH ⁺	1.300 ± 0.702	2.420 ± 0.575	10.377 ± 4.521	23.617 ± 20.086	1.115 ± 0.343
Elemental Species (mg kg⁻¹)	31.586 ± 10.630	29.265 ± 4.240	51.062 ± 5.920	16.738 ± 3.480	11.817 ± 6.650
Phenols (mg kg⁻¹)	20.774 ± 4.972	13.193 ± 2.181	20.480 ± 1.403	23.521 ± 8.521	7.689 ± 1.356
PAHs (mg kg⁻¹)	1.257 ± 0.398	1.420 ± 0.232	3.967 ± 0.970	4.359 ± 1.373	1.123 ± 0.205

1649

ND means not detected

Table 3. Comparison of emission factors with literature (specific chemical materials in form of PM_{2.5}).

Species	Emission factors (g kg ⁻¹)		Reference
	This work	Reference value	
PM _{2.5}	8.99 ± 5.55	7.6~11.7(AR), 6.26~15.3 (TL), ~3.0 (AR), 2.2~15.0 (AR)	Li et al., 2007; Akagi et al., 2011; Dhammapala et al., 2007; Hayashi et al., 2014
PM _{1.0}	7.91 ± 4.67	4.4.3~12.1 (TL)	May et al., 2014
OC	4.21 ± 2.73	2.7~3.9 (AR), 2.3~9.7(TL), ~1.9(AR) , 1.0~9.3 (AR), 0.8~5.9 (TL)	Li et al., 2007; Akagi et al., 2011; Dhammapala et al., 2007; Hayashi et al., 2014; May et al., 2014
EC	1.09 ± 0.65	0.35~0.49 (AR), 0.37~0.91(TL), ~0.4(AR), 0.21~0.81(AR), 1.13~1.73 (TL)	Li et al., 2007; Akagi et al., 2011; Dhammapala et al., 2007; Hayashi et al., 2014; May et al., 2014
WSOA	0.33 ± 0.31	0.039~0.109 (TL)	Akagi et al., 2011
WSA	0.05 ± 0.05	0.08~0.13 (TL), ~0.55 (TL)	Akagi et al., 2011; Andreae et al., 2001
WSI	2.10 ± 1.34	1.84~4.9 (AR),0.8~1.31(TL), 0.43~1.63 (AR)	Li et al., 2007; Akagi et al., 2011; Hayashi et al., 2014
THM	0.06 ± 0.05	0.06~0.09 (AR)	Li et al., 2007
PAHs (×10 ³)	4.38 ± 3.15	~17(AR), 0.72~1.64(AR), ~9.0 (W)	Dhammapala et al., 2007; Zhang et al., 2011; Lee et al.2005
Phenols (×10 ³)	24.31 ± 12.11	~35(AR), ~5 (AR), ~13 (TL)	Dhammapala et al., 2007; Hays et al., 2005; Andreae et al., 2001

AR: agricultural residue; TL: total, including forest fires and straw burning; W: wood

Table 4. Summary of field burning rates and economic data in China.

Province	Burning rate from literature		Agricultural income ratio ^c			Estimated burning rate		NDRC report ^d	Average rate
	BAU-I ^a	BAU-II ^b	2000	2006	2012	EM-I	EM-II	NDRC	
Beijing	0.00	0.17	0.08	0.06	0.06	0.00	0.19	0.13	0.10 ±0.08
Tianjin	0.00	0.17	0.10	0.14	0.12	0.00	0.20	0.30	0.13 ±0.12
Hebei	0.20	0.17	0.27	0.22	0.24	0.22	0.16	0.19	0.19 ±0.02
Shanxi	0.20	0.17	0.20	0.21	0.25	0.16	0.14	0.22	0.18 ±0.03
Inner Mongolia	0.00	0.12	0.44	0.49	0.66	0.00	0.09	0.27	0.10 ±0.10
Liaoning	0.20	0.12	0.30	0.29	0.39	0.16	0.09	0.34	0.18 ±0.09
Jilin	0.30	0.12	0.73	0.73	0.77	0.28	0.11	0.25	0.21 ±0.08
Heilongjiang	0.30	0.12	0.99	0.83	0.59	0.50	0.17	0.25	0.27 ±0.13
Shanghai	0.00	0.32	0.10	0.08	0.09	0.00	0.29	0.12	0.15 ±0.14
Jiangsu	0.30	0.32	0.32	0.22	0.30	0.32	0.23	0.19	0.27 ±0.05
Zhejiang	0.30	0.32	0.19	0.08	0.09	0.64	0.28	0.22	0.35 ±0.15
Anhui	0.20	0.32	0.44	0.39	0.43	0.21	0.29	0.43	0.29 ±0.08
Fujian	0.30	0.32	0.18	0.10	0.14	0.39	0.22	0.17	0.28 ±0.08
Jiangxi	0.20	0.11	0.45	0.31	0.44	0.20	0.08	0.25	0.17 ±0.06
Shandong	0.30	0.17	0.33	0.25	0.24	0.40	0.17	0.21	0.25 ±0.09
Henan	0.20	0.17	0.39	0.35	0.33	0.23	0.18	0.22	0.20 ±0.02
Hubei	0.20	0.11	0.42	0.30	0.41	0.21	0.08	0.30	0.18 ±0.08
Hunan	0.20	0.33	0.47	0.31	0.43	0.22	0.24	0.35	0.27 ±0.06
Guangdong	0.30	0.33	0.19	0.10	0.13	0.44	0.25	0.18	0.30 ±0.09
Guangxi	0.20	0.33	0.40	0.25	0.33	0.25	0.25	0.35	0.28 ±0.06
Hainan	0.30	0.33	0.35	0.16	0.21	0.51	0.25	0.56	0.39 ±0.12
Chongqing	0.20	0.11	0.35	0.23	0.30	0.24	0.08	0.45	0.22 ±0.13
Sichuan	0.20	0.11	0.37	0.22	0.28	0.26	0.09	0.30	0.19 ±0.08
Guizhou	0.20	0.11	0.38	0.23	0.25	0.31	0.10	0.43	0.23 ±0.13
Yunnan	0.20	0.11	0.36	0.26	0.31	0.24	0.09	0.28	0.18 ±0.07
Tibet	0.00	0.16	0.15	0.09	0.05	0.00	0.30	0.16	0.12 ±0.11
Shannxi	0.20	0.17	0.33	0.27	0.26	0.25	0.18	0.28	0.22 ±0.04
Gansu	0.10	0.16	0.25	0.20	0.28	0.09	0.11	0.33	0.16 ±0.09
Qinghai	0.00	0.16	0.23	0.10	0.08	0.00	0.20	0.28	0.13 ±0.11
Ningxia	0.10	0.16	0.42	0.38	0.45	0.09	0.13	0.16	0.13 ±0.03
Xinjiang	0.10	0.16	0.43	0.61	0.73	0.06	0.13	0.30	0.15 ±0.08
Nationwide	0.21	0.16	0.34	0.27	0.31	0.26	0.15	0.27	0.21 ±0.05

a. Zhao et al., 2012; Cao et al., 2006; Cao et al., 2011

b. Wang and Zhang., 2008

c. Calculated based on data from China Yearbook 2001~2013 (NBSC, 2001-2013), China Rural Statistic Yearbook 2001~2013, data available at <http://www.grain.gov.cn/Grain/>

d. Data from the National Development and Reform Commission report ([2014]No.516) : <http://www.sdpc.gov.cn/>

Table 5. National agricultural field burning emissions of BAU, EM, and NDRC scenarios in China in 2012.

Unit: Gg	BAU-I			BAU-II			EM-1			EM-2			NDRC			Average		
	Total	Summer	Autumn	Total	Summer	Autumn	Total	Summer	Autumn	Total	Summer	Autumn	Total	Summer	Autumn	Total	Summer	Autumn
PM _{2.5}	1001.05	218.99	782.06	835.42	209.29	626.13	1211.92	258.58	953.34	738.36	182.34	556.02	1241.69	258.24	983.46	1007.650	226.007	781.646
PM _{1.0}	897.52	198.93	698.59	748.57	189.92	558.65	1087.05	234.85	852.20	661.81	165.61	496.20	1111.90	234.44	877.46	903.125	205.217	697.911
OC	429.51	102.87	326.64	360.99	97.67	263.32	519.26	121.33	397.94	318.84	85.55	233.29	533.19	120.86	412.33	433.184	105.885	327.300
EC	133.61	27.37	106.24	111.40	26.52	84.88	162.71	32.39	130.32	98.06	22.85	75.21	164.97	32.53	132.45	134.414	28.404	106.010
SO ₄ ²⁻	30.22	3.96	26.26	24.97	3.94	21.04	36.39	4.71	31.68	22.09	3.32	18.76	38.21	4.78	33.44	30.440	4.155	26.285
NO ₃ ⁻	4.35	0.84	3.51	3.55	0.80	2.75	5.24	0.99	4.25	3.17	0.70	2.47	5.40	0.99	4.41	4.350	0.864	3.486
NH ₄ ⁺	32.08	6.37	25.71	26.65	6.21	20.44	39.09	7.54	31.55	23.43	5.32	18.11	39.46	7.59	31.87	32.202	6.623	25.580
K ⁺	67.49	13.12	54.38	54.75	12.38	42.37	81.40	15.45	65.95	49.10	10.90	38.20	83.62	15.36	68.26	67.412	13.469	53.943
WSOA	24.44	6.55	17.89	21.94	6.39	15.55	29.69	7.76	21.93	18.77	5.48	13.30	30.82	7.81	23.01	25.174	6.815	18.360
WSA	5.75	0.95	4.80	4.85	0.95	3.90	6.99	1.13	5.86	4.23	0.80	3.43	7.19	1.15	6.04	5.815	1.000	4.815
PAHs	0.48	0.11	0.37	0.40	0.10	0.30	0.58	0.12	0.45	0.35	0.09	0.26	0.59	0.13	0.47	0.480	0.109	0.371
Phenols	2.71	0.85	1.87	2.25	0.78	1.47	3.25	0.99	2.26	2.02	0.70	1.323	3.40	0.98	2.36	2.721	0.861	1.861
THM	8.68	2.01	6.67	7.19	1.92	5.27	10.56	2.37	8.19	6.36	1.67	4.69	10.64	2.37	8.27	8.702	2.073	6.628
WSI	249.96	47.46	202.50	204.46	45.24	159.22	301.75	56.01	245.74	182.31	39.50	142.82	310.31	55.88	254.43	250.269	48.927	201.342

Table 6. Uncertainties for the national smoke aerosol emissions in 2012 (pollutant emission in unit of Gg/yr, 95% CI in percentage)

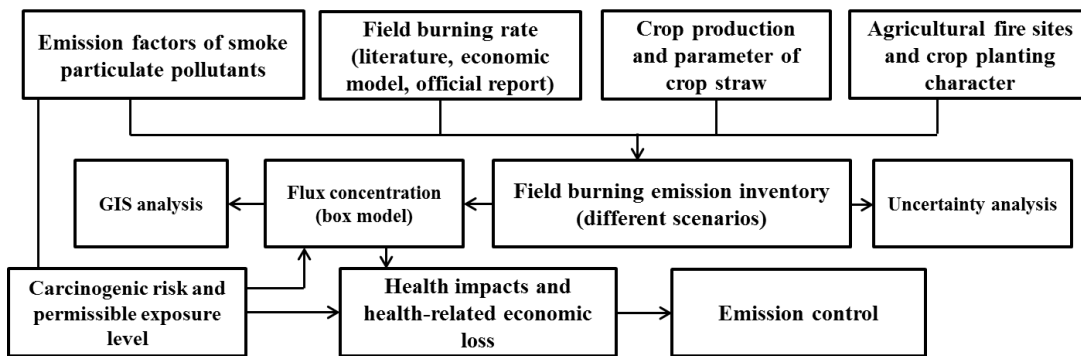
Species	BAU-I		BAU-II		EM-I		EM-II		NDRC		Average	
PM _{2.5}	1001.1	(-52.3% , 73.5%)	835.4	(-48.7% , 68.8%)	1211.9	(-63.6% , 84.3%)	738.4	(-55.9% , 74.3%)	1241.7	(-46.2% , 65.1%)	1005.7	(-24.6% , 33.7%)
PM _{1.0}	897.5	(-51.6% , 73.0%)	748.6	(-48.4% , 68.6%)	1087.1	(-62.9% , 83.8%)	661.8	(-55.5% , 74.1%)	1111.9	(-45.7% , 64.7%)	901.4	(-24.4% , 33.5%)
OC	429.5	(-50.5% , 71.5%)	361.0	(-48.9% , 69.2%)	519.3	(-61.4% , 81.8%)	318.8	(-55.6% , 74.1%)	533.2	(-47.1% , 66.7%)	432.4	(-24.2% , 33.3%)
EC	133.6	(-52.1% , 73.6%)	111.4	(-50.1% , 71.0%)	162.7	(-63.3% , 84.3%)	98.1	(-56.8% , 75.7%)	165.0	(-46.7% , 66.0%)	134.2	(-24.8% , 34.0%)
WSOA	24.4	(-68.5% , 86.2%)	21.9	(-75.7% , 95.2%)	29.7	(-78.7% , 96.2%)	18.8	(-77.8% , 95.4%)	30.8	(-67.5% , 85.1%)	25.1	(-33.3% , 41.4%)
WSA	5.8	(-62.8% , 82.1%)	4.9	(-65.9% , 84.1%)	7.0	(-73.9% , 93.2%)	4.2	(-69.3% , 86.3%)	7.2	(-58.7% , 75.9%)	5.8	(-30.1% , 38.5%)
WSI	250.0	(-54.4% , 77.2%)	204.5	(-47.5% , 67.4%)	301.8	(-66.9% , 89.3%)	182.3	(-56.1% , 74.8%)	310.3	(-46.9% , 66.4%)	249.8	(-25.4% , 34.9%)
THM	8.7	(-56.2% , 77.5%)	7.2	(-52.8% , 71.4%)	10.6	(-67.5% , 88.3%)	6.4	(-61.2% , 79.5%)	10.6	(-50.8% , 69.4%)	8.7	(-26.6% , 35.6%)
PAHs	0.5	(-55.2% , 75.7%)	0.4	(-52.4% , 72.2%)	0.6	(-66.5% , 86.8%)	0.4	(-58.8% , 76.9%)	0.6	(-49.3% , 67.8%)	0.5	(-26.0% , 34.9%)
Phenols	2.7	(-56.1% , 77.6%)	2.3	(-51.4% , 70.6%)	3.3	(-67.3% , 88.3%)	2.0	(-59.9% , 78.4%)	3.4	(-48.7% , 67.1%)	2.7	(-26.1% , 35.1%)

Table 7. Estimated number of cases (95% CI) attributable to agricultural fire smoke PM_{2.5} exposure in China, 2012.

Emission version	Mortality	Respiratory hospital admission	Cardiovascular hospital admission	Chronic bronchitis
BAU-I	7864 (3154, 12489)	31123 (21114, 40788)	29454 (12849, 45481)	7577067 (2952006, 11024705)
BAU-II	7187 (3056, 11260)	28711 (19443, 37693)	27156 (11825, 42007)	7132581 (2735111, 10523803)
EM-I	9435 (3817, 14933)	36950 (25151, 48269)	35116 (15373, 54042)	8712880 (3484325, 12430411)
EM-II	6175 (2554, 9751)	25166 (17004, 33112)	23745 (10316, 36816)	6383442 (2407643, 9526727)
NDRC	8523 (3581, 13377)	33957 (23015, 44542)	32131 (14003, 49664)	8332216 (3228351, 12148274)
Average	7836 (3232, 12362)	31181 (21145, 40881)	29520 (12873, 45602)	7267237 (2961487, 1130784)
CRC	538 (227, 850)	2191 (1462, 2920)	2038 (874, 3199)	636650 (214617, 1052153)

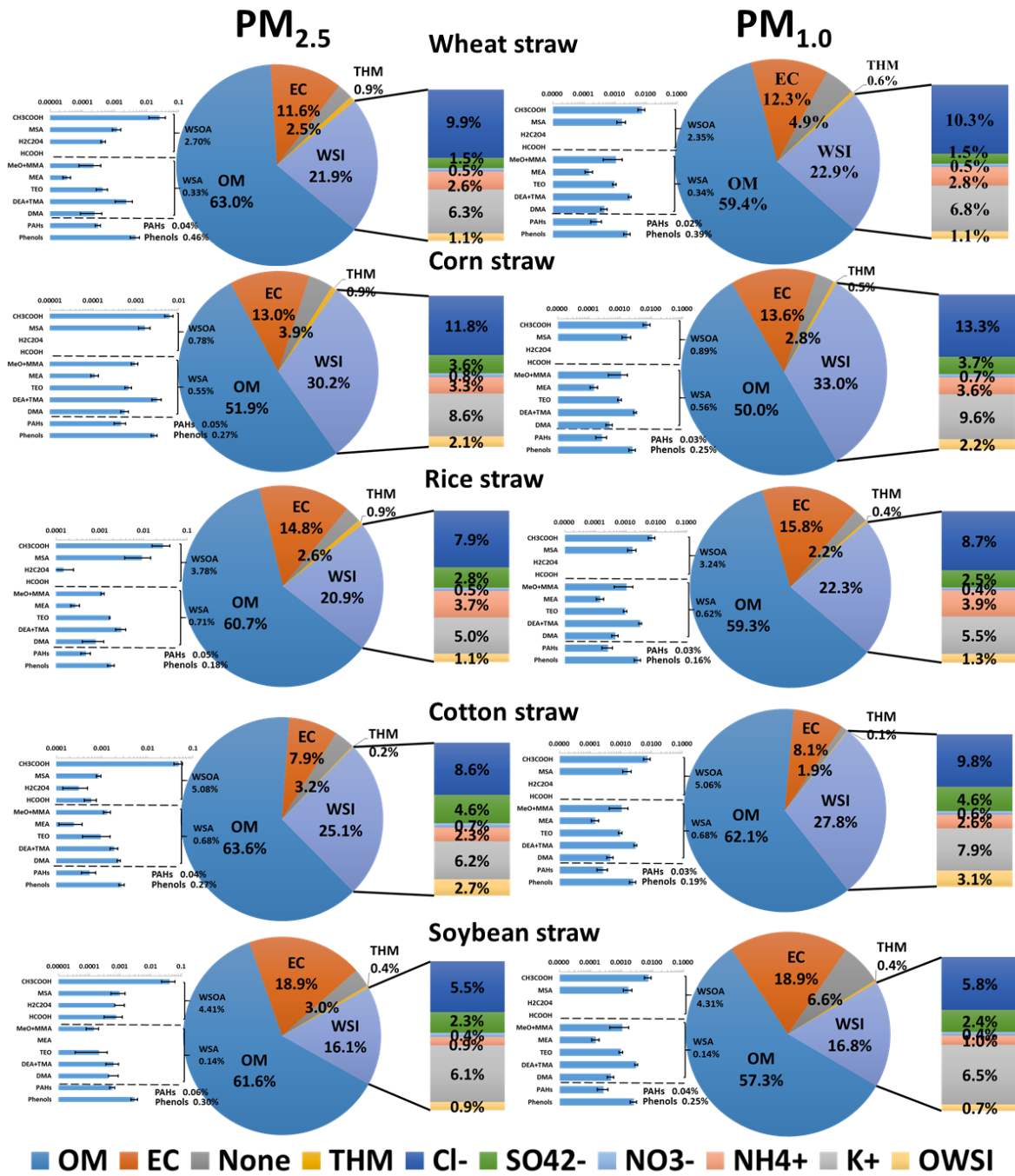
Table 8. Health-related economic loss (95% CI) from agricultural fire smoke PM_{2.5} exposure in China, 2012.

Emission version	Economic cost (million US\$)				Total cost (million US\$)	GDP ratio (‰)
	Mortality	Respiratory hospital admission	Cardiovascular hospital admission	Chronic bronchitis		
BAU-1	1544.5 (730.7, 2430.0)	19.6 (13.3, 25.7)	36.0 (15.7, 55.6)	7187.6 (2800.3, 10458.3)	8787.8 (3560.0, 12969.4)	1.0 (0.4 , 1.5)
BAU-2	1453.9 (719, 2252.2)	18.1 (12.2, 23.8)	33.2 (14.4, 51.3)	6766.0 (2594.5, 9982.9)	8271.2 (3340.3, 12310.3)	1.0 (0.4 , 1.4)
EM-1	1855.2 (870.3, 2913.7)	23.3 (15.9, 30.5)	42.9 (18.8, 66.1)	8265.0 (3305.2, 11791.5)	10186.5 (4210.2, 14801.8)	1.2 (0.5 , 1.7)
EM-2	1228.1 (600.6, 1917.6)	15.9 (10.7, 20.9)	29.0 (12.6, 45.0)	6055.3 (2283.9, 9037.1)	7328.4 (2907.9, 11020.7)	0.9 (0.3 , 1.3)
NDRC	1573.4 (759.3, 2456.2)	21.4 (14.5, 28.1)	39.3 (17.1, 60.7)	7903.9 (3062.4, 11523.9)	9538.2 (3853.4, 14069.0)	1.1 (0.4 , 1.6)
Average	1531.0 (736.0, 2393.9)	19.7 (13.3, 25.8)	36.1 (15.7, 55.7)	7235.6 (2809.3, 10558.7)	8822.4 (3574.4, 13034.2)	1.0 (0.4 , 1.5)
CRC	100.0 (48.0, 157.1)	1.3 (0.9, 1.8)	2.4 (1.0, 3.9)	603.9 (203.6, 998.1)	707.8 (253.6, 1160.9)	0.1 (0.0 , 0.1)



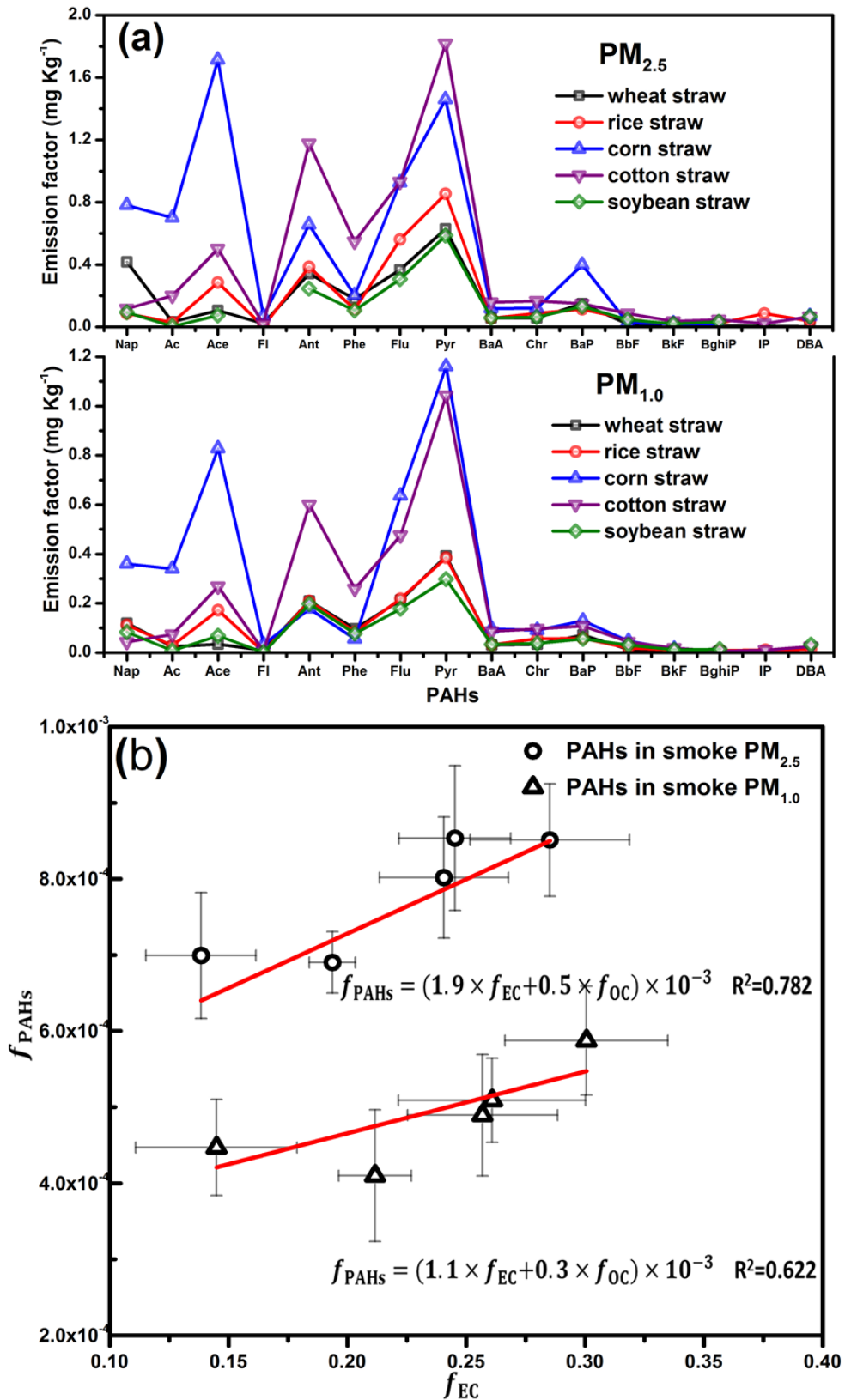
1
2
3

Figure 1. Schematic methodology for developing emission estimations.



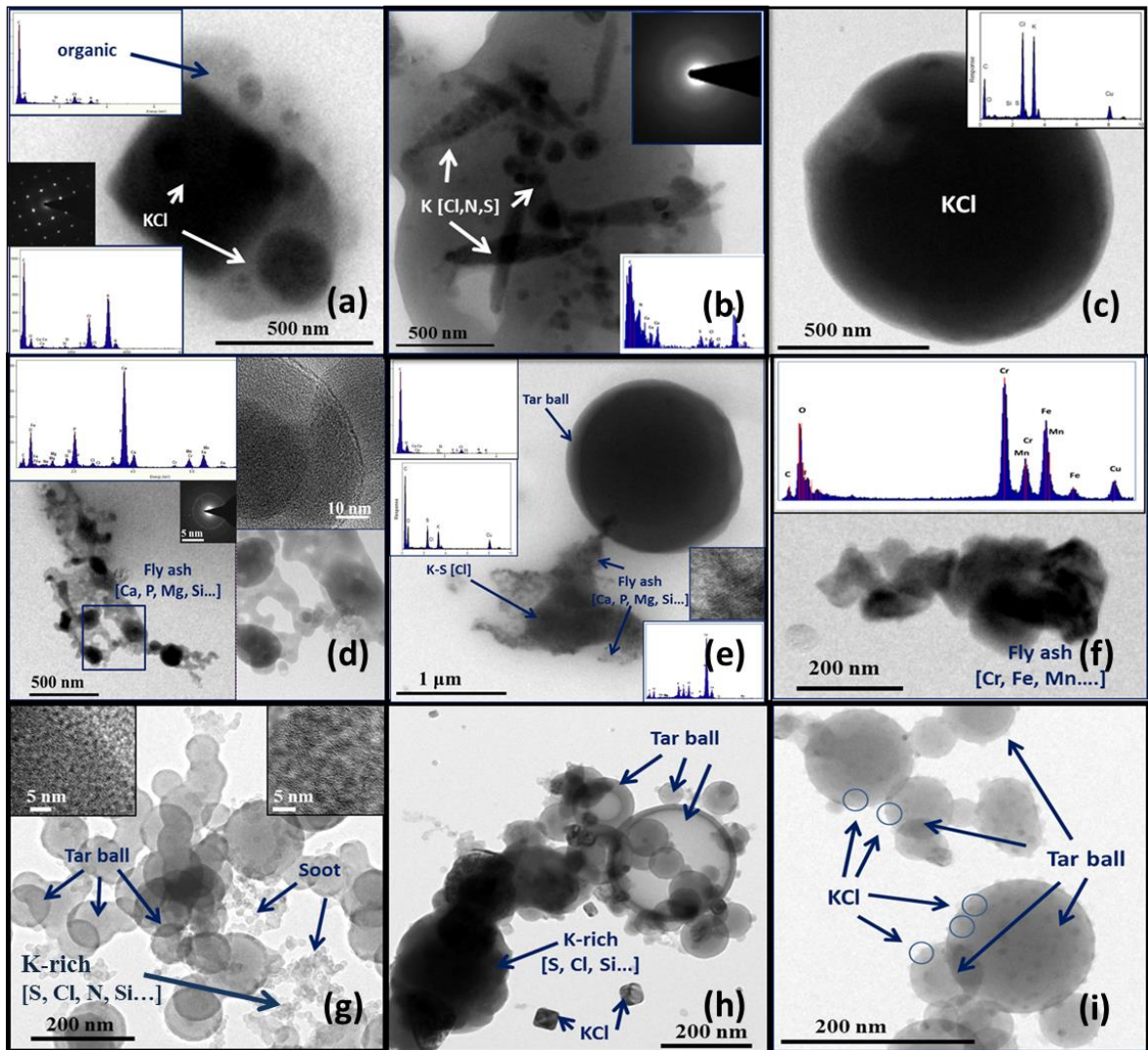
5

6 **Figure 2.** Chemical profiles of smoke PM_{2.5} and PM_{1.0} from 5 types agricultural
 7 residue burnings. OM (organic matter = 1.3×OC). OWSI, other water soluble ions
 8 including F⁻, NO₂⁻, Na⁺, Ca²⁺, and Mg²⁺.



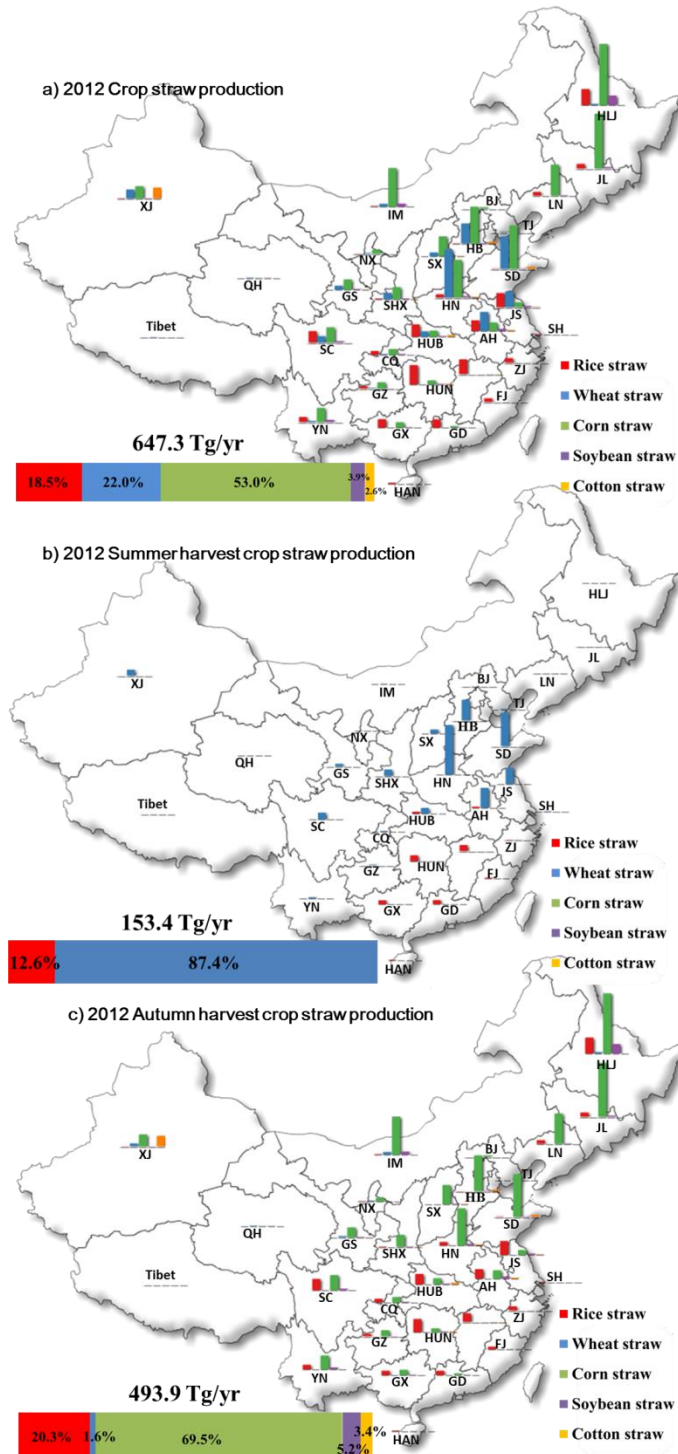
9
10
11
12

Figure 3. (a) Emission factors of 16 USEPA priority PAHs in smoke PM_{2.5} and PM_{1.0};
(b) expulsion-accumulation of PAHs in OC-EC of smoke PM_{2.5} and PM_{1.0}.



13
 14 **Figure 4.** Transmission electron microscope (TEM) images and EDX analysis of
 15 fresh agricultural residue burning particles. (a)-(c) Crystal and amorphous KCl
 16 particles internally mixed with sulfate, nitrate, and carbonaceous materials. (d)-(f)
 17 Heavy metal-bearing fractal-like fly ash particles. (e)-(g) Chain-like soot particles and
 18 tar ball.

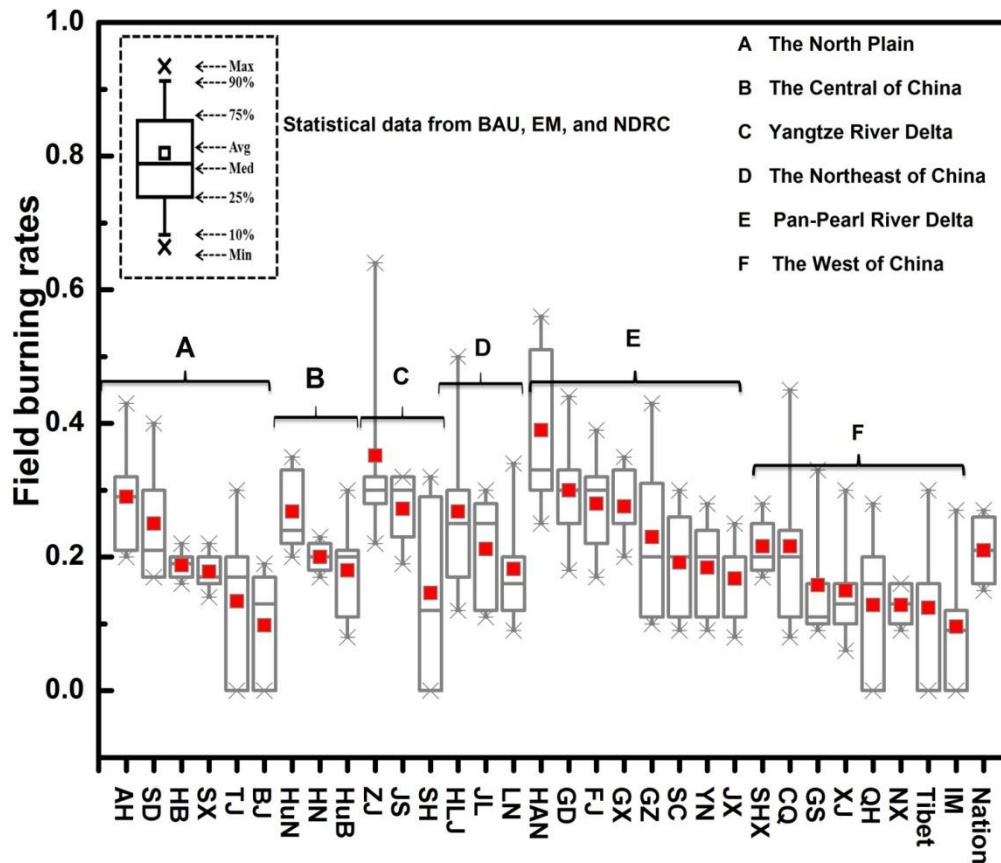
19



20

21 **Figure 5.** Annual agricultural residue production of five major crops and allocated
 22 into two harvest (summer and autumn harvest) based on agricultural yield in China,
 23 2012. (Abbreviation, BJ: Beijing; TJ: Tianjin; HB: Hebei; SX: Shanxi; IM: Inner Mongolia; LN: Liaoning; JL:
 24 Jilin; HLJ: Heilongjiang; SH: Shanghai; JS: Jiangsu; ZJ: Zhejiang; AH: Anhui; FJ: Fujian; JX: Jiangxi; SD:
 25 Shandong; HN: Henan; HUB: Hubei; HUN: Hunan; GD: Guangdong; GX: Guangxi; HAN: Hainan; CQ:
 26 Chongqing; SC: Sichuan; GZ: Guizhou; YN: Yunnan; SHX: Shannxi; GS: Gansu; QH: Qinghai; NX: Ningxia; XJ:
 27 Xinjiang)

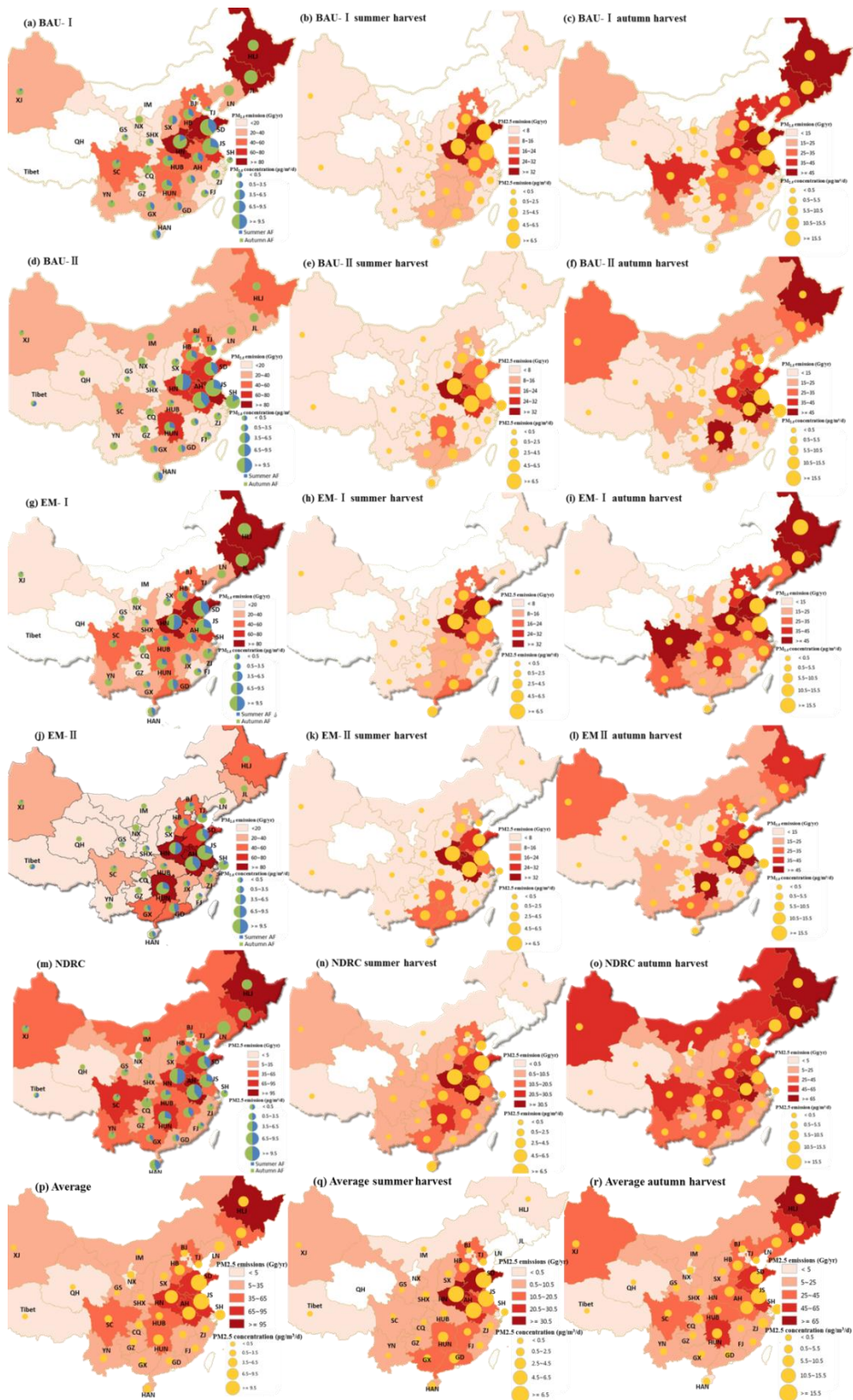
28



29

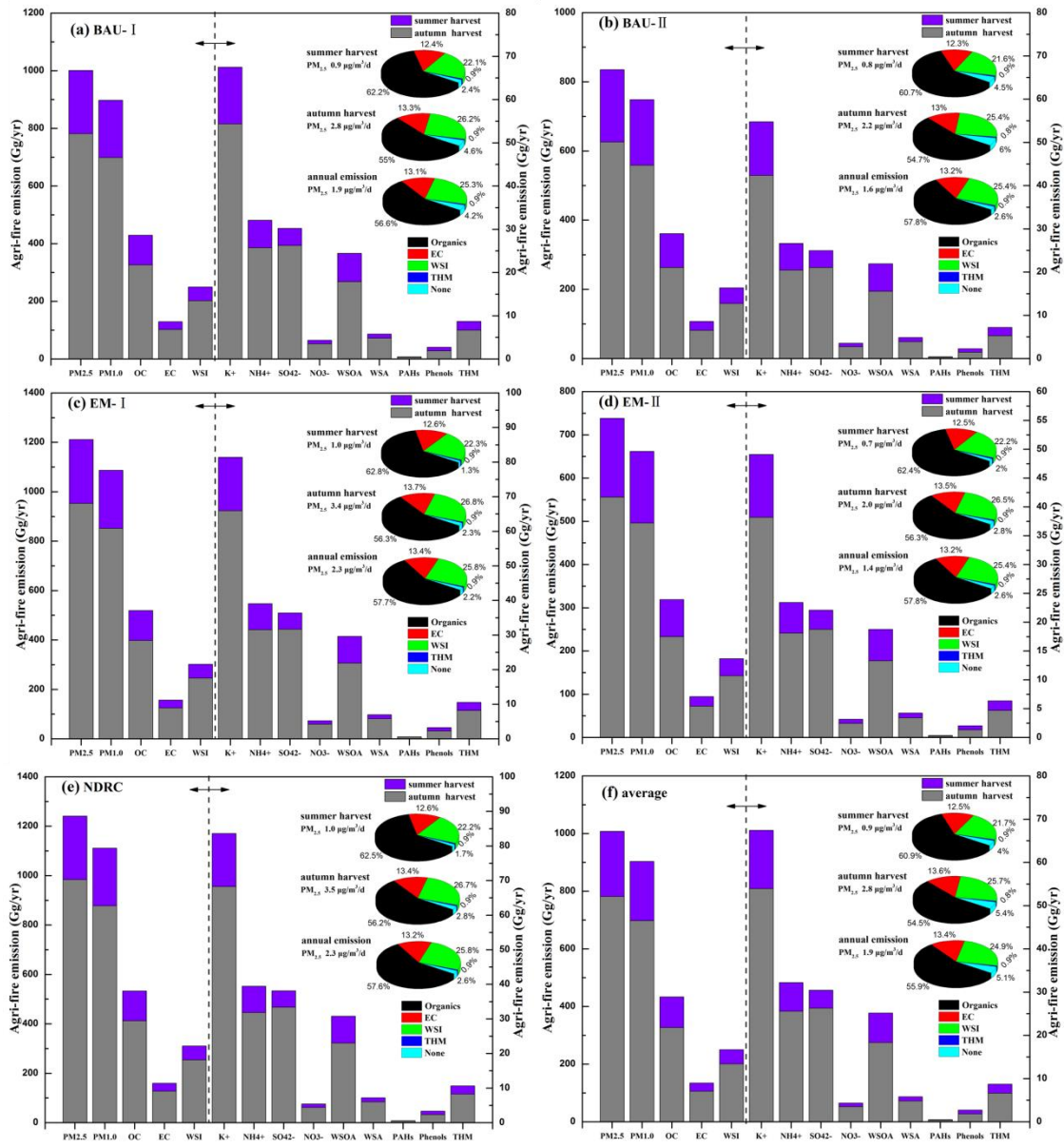
30 **Figure 6.** Statistical analysis of field burning rates from BAU, EM, and NDRC
 31 versions. The North Plain (Anhui, Shandong, Hebei, Shanxi, Tianjin, Beijing), the
 32 Central of China (Hunan, Henan, Hubei), the Yangtze River Delta (Zhejiang, Jiangsu,
 33 Shanghai), the Northeast of China (Heilongjiang, Liaoning, Jilin), the Pan-Pearl River
 34 Delta (Hainan, Guangdong, Fujian, Guangxi, Guizhou, Sichuan, Yunnan, Jiangxi), the
 35 West of China (Shannxi, Chongqing, Xinjiang, Qinghai, Ningxia, Tibet, Inner
 36 Mongolia, Gansu)

37



38

39 **Figure 7.** Spatial and temporal distribution of smoke PM_{2.5} emissions and flux
 40 concentrations from agricultural field burning over China, 2012.



41

42 **Figure 8.** Nationwide $PM_{2.5}$ emissions and flux concentrations based on different
 43 burning versions. The inset pie-graphs are chemical compositions of integrated $PM_{2.5}$
 44 from five major agricultural residue burning.